

**DEVELOPMENT AND EVALUATION OF THE QUINTESSENTIAL VENTRICULAR
CANNULA**

by

Timothy Nicholas Bachman

BS, University of Pittsburgh, 2004

Submitted to the Graduate Faculty of
Swanson School of Engineering in partial fulfillment
of the requirements for the degree of
Master of Science

University of Pittsburgh

2008

UNIVERSITY OF PITTSBURGH
SWANSON SCHOOL OF ENGINEERING

This thesis was presented

by

Timothy Nicholas Bachman

It was defended on

March 20th, 2008

and approved by

Harvey S. Borovetz, Ph.D., Department of Bioengineering

Robert L. Kormos, MD, Department of Surgery

Thesis Advisor: James F. Antaki, Ph.D., Department of Bioengineering

Copyright © by Timothy Nicholas Bachman

2008

DEVELOPMENT AND EVALUATION OF THE QUINTESSENTIAL VENTRICULAR CANNULA

Timothy Nicholas Bachman, MS

University of Pittsburgh, 2008

Left Ventricular Assist Devices (LVADs) are becoming a more widely accepted form of treatment for patients suffering from end stage heart failure. First generation LVADs attempted to mimic the physiology of the native heart by generating pulsatile blood flow. Second- and third-generation turbodynamic LVADs are much smaller than pulsatile LVADs, but alternatively generate non-physiologic continuous flow.

A vast amount of time and resources have been spent on optimizing the hemodynamics LVADs. One area that has changed very little, however, is the apical cannula- an inflow conduit that is inserted into the apex of the left ventricle (LV) allowing blood to be drawn from the LV chamber by the LVAD so that the heart can be effectively unloaded. Current inflow cannulae are often straight rigid tubes which extend far into the LV, and are susceptible to becoming displaced during the implantation of the device or post-operatively. A malpositioned cannula may cause reduced flow, it may interfere with ventricular anatomy, and it may generate areas of stagnation that can form thrombus. Additionally, the advent of continuous flow LVADs brought about a new problem where the negative pressures generated within the ventricle by the LVAD can cause the chamber to collapse. A sub-optimally placed cannula may increase the likelihood of these suction events.

An ongoing collaborative effort at the University of Pittsburgh and Carnegie Mellon University has resulted in the design of a more robust low-profile cannula. The design is intended to minimize variations in pump output by reducing the cannula's ability to be malpositioned. This reduces interactions with ventricular anatomy, and is more likely to generate hemodynamically favorable flow. This design is also intended to reduce the likelihood of ventricular collapse across the spectrum of physiologic conditions by providing mechanical support for the ventricular wall.

In-silico and ex-vivo studies, including in-situ visualization of ventricular suction in an arrested ovine ventricle, demonstrated that the novel cannula design is indeed a more robust design, and more compatible with ventricular anatomy. Further development of the flared inflow cannula is warranted, as is the study of its interaction with the left ventricle under sub-optimal conditions.

TABLE OF CONTENTS

PREFACE.....	XIV
1.0 INTRODUCTION.....	1
1.1 CARDIAC FUNCTION, FAILURE, AND TREATMENT.....	1
1.1.1 Human Cardiac Physiology.....	1
1.1.2 Heart Failure	3
1.1.3 Ventricular Assist Devices.....	3
1.1.4 Current cannula options.....	6
1.1.5 Need for Improved Inflow Cannula	6
1.2 PREVIOUS CANNULA DESIGN EFFORTS AT THE UNIVERISTY OF PITTSBURGH	8
1.2.1 Antaki et al.....	8
1.2.2 Curtis et al.....	10
2.0 CANNULA DEVELOPMENT	12
2.1 DESIRED CANNULA FEATURES	12
2.1.1 Attachment	12
2.1.2 Geometry.....	12
2.1.2.1 Hemodynamics.....	12
2.1.2.2 Anatomic Fit.....	13
2.1.3 Materials	13
2.1.3.1 Mechanical Properties.....	13

2.1.3.2	Biocompatibility	13
2.2	QVC CANNULA	14
3.0	CANNULA EVALUATION	16
3.1	ANATOMIC FIT STUDIES	16
3.1.1	In-silico	16
3.1.1.1	Methods	17
3.1.1.2	Results	22
3.1.1.3	Discussion	23
3.1.2	Ex-vivo	25
3.1.2.1	Methods	25
3.1.2.2	Results	26
3.2	CANNULA PULLOUT STUDY	27
3.2.1	Description of study	27
3.2.2	Methods	27
3.2.2.1	Preparation of myocardium	27
3.2.2.2	Supporting the myocardium and placement of cannula	28
3.2.2.3	Force application, measurement, and data acquisition	28
3.2.2.4	Experimental Procedure	28
3.2.3	Results	30
3.3	VENTRICULAR SUCTION STUDY	31
3.3.1	Description of study	31
3.3.2	Methods	31
3.3.2.1	Experimental setup	31
3.3.2.2	Experimental procedure	34
3.3.2.3	Analysis	36

3.3.3	Results	37
3.3.4	Discussion.....	47
4.0	CONCLUSIONS	49
4.1	PROPOSED MODIFICATIONS OF CANNULA	50
4.1.1	Facilitation of Hemostasis	50
4.1.2	Sizing	50
4.2	CONTRAINDICATIONS FOR USE.....	51
4.3	FUTURE STUDIES.....	51
APPENDIX A		52
BIBLIOGRAPHY		56

LIST OF TABLES

Table 1-Modes of collapse which occurred for each setting	40
Table 2-Assumed values and resulting Reynolds numbers for cannulae	45

LIST OF FIGURES

Figure 1-(Top) The Streamliner Axial Flow Ventricular Assist Device. (Bottom left) Reconstruction generated from a CT scan of a patient with a pulsatile HeartMate XVE LVAD. (Bottom Right) Reconstruction generated from a CT scan of a patient with an axial flow HeartMate II LVAD.....	5
Figure 2- Traditional inflow cannula tip geometries: (L-R) blunt, beveled, caged. The caged cannula is more commonly used for atrial cannulation.	6
Figure 3-Trumpet mouth cannula tip introduced by Antaki et al	9
Figure 4-(Left) Dissected LV with trumpet cannula. (Middle) Thrombus produced by blood flow at tip of cage. (Right) A malpositioned cannula with entrained papillary muscle. And large thrombus formed at the apex, where blood has stagnated.	9
Figure 5- In-vitro setup used for visualizing the flow within the cannulated ventricle casts	10
Figure 6-Flow visualization of performed by Curtis et al. using various cannula geometries in transparent bovine LV casts: (Top left) beveled; (Top middle) beveled with side vent; (Top right) caged; (Bottom left) blunt; (bottom right) trumpet tip. The red circles indicate areas of stagnation or recirculation; the yellow and white lines are intended to help clarify the boundaries of the cannula and ventricle wall respectively. (Note: the large bright spots at the top of each ventricle are from the laser reflecting off of the wall, and should not be interpreted as collecting particles).....	11
Figure 7- (left) Iterations of the QVC. (Right)Section view of final flared design	14
Figure 8- The high memory polymer used to fabricate the QVC allowed it to be folded and compressed in order to facilitate easy insertion into the LV	15
Figure 9- the QVC deployed through a piece of acrylic. The diameter of the flare, far exceeds the diameter through which it has been inserted.....	15
Figure 10- (Top Left) Initial CT scan of chest, imported into Mimics. (Top Right) CT scan with enhanced contrast. (Bottom) Image was resliced along long axis (red line) in order to obtain short axis view of LV.....	18
Figure 11- Segmented LV.....	19

Figure 12- removal of artifacts	19
Figure 13- Manual editing of reconstruction in Mimics. The yellow arrows indicate the papillary muscles and the yellow circles indicate the resulting undercuts in the reconstructed blood-occupied volume. The red arrow shows where detail such as trabeculae have been omitted in order to reduce noise.....	20
Figure 14- Point cloud imported from Mimics into Geomagics.....	21
Figure 15-Polygonal surface	21
Figure 16- Polygonal surface following noise reduction.....	22
Figure 17-(Left) Grid generated on surface. (Middle) Mesh fit within grid. (Right) Resulting Surface than can be exported to CAD programs	22
Figure 18- (Top Left) CAD surface at end-diastole. (Bottom Left) CAD surface at end-systole. (Right) Usage of the CAD surface to analyze the interaction of the QVC with the LV anatomy.....	23
Figure 19- Changes in elevation generated during end diastolic surface noise reduction.....	24
Figure 20- Changes in elevation generated during end systolic surface noise reduction.	25
Figure 21-(top) properly placed QVC design. (Middle) external view of torqued cannula. (Bottom) internal view of torqued cannula.....	26
Figure 22-(Left) nominally placed beveled cannula. (Right) Slightly torqued beveled cannula now pointed towards ventricular wall.....	27
Figure 23- (Left) top view of supported and cannulated section. (Right) bottom view of same section.	29
Figure 24- The test setup consists of a container hung from a cannula, attached to a supported section of myocardium, which transfers the force applied to the cannula to the load cell.	29
Figure 25- This graph illustrates that the force was increased at the same constant rate for each test. The peak and sudden drop in force also indicates the maximum force immediately prior to being pulled from the myocardium. Force does not equal zero at time zero, because the water container was hung from the cannula prior to commencement of data logging.	30
Figure 26- Diagram of suction setup	33
Figure 27-Ovine Heart Preparation: (Top-Left) Pericardial sac removed; (Bottom-Left) Left atrium dissected; (Middle) T-tube inserted and tied with purse string; (Right) drawing of the components that were assembled to create a leak-proof t-tube connector.....	33

Figure 28-Loop setup showing borescope, cannulated LV, and direction of flow (indicated by arrow).....	34
Figure 29- The beveled cannula (white) and the QVC (blue)	35
Figure 30-- (Left) Properly positioned cannula. (Right) Intentionally malpositioned cannula. ...	35
Figure 31-Particle flow fields generated at a patent beveled cannula inlet (left) and deposition surrounding a malpositioned beveled cannula (right).....	40
Figure 32-Still images captured from borescopic video which illustrate the progression of the various modes of suction that occurred during the study.	41
Figure 33- Still images acquired from the simulation of hypovolemia	42
Figure 34-Still images of the over-pumping simulation.....	43
Figure 35- Pressure versus flow during the hypovolemic simulation in second study with pump speed fixed to 1250 RPM.....	44
Figure 36- Flow versus speed data for properly and improperly placed cannula during the over-pumping simulation in second study at a fixed initial LAP of 20mmHg.	44
Figure 37-Percentage change in flow for the hypovolemic simulation in second study at a fixed speed of 1250 RPM.....	45
Figure 38- Percent change in maximal attainable flow (regardless of speed) measured during the over-pumping simulation of the second study.....	46
Figure 39- Examples of the progression of the data acquired during a test run (study attempt #2). (Left) Progression of a hypovolemic study, concluding with an oscillation. (Right) Progression of an over-pumping study.	46
Figure 40-Examples of variations of Oscillation. (Left) incomplete occlusion with dampening. (Right) Total occlusion.	47
Figure 41-Pressure versus flow during the hypovolemic simulation in second study with pump speed fixed to 1500 RPM.....	53
Figure 42-Pressure versus flow during the hypovolemic simulation in second study with pump speed fixed to 1750 RPM.....	53
Figure 43-Flow versus speed data for properly and improperly placed cannula during the over-pumping simulation in second study at a fixed initial LAP of 15mmHg	54
Figure 44-Flow versus speed data for properly and improperly placed cannula during the over-pumping simulation in second study at a fixed initial LAP of 10mmHg	54

Figure 45-Percentage change in flow for the hypovolemic simulation in second study at a fixed speed of 1500 RPM.....	55
Figure 46-Percentage change in flow for the hypovolemic simulation in second study at a fixed speed of 1750 RPM.....	55

PREFACE

If all of those who offered encouragement, insight, or well wishes were listed in this section, its size would far exceed that of the rest of this document. So, to all those who I have met throughout this amazing journey, I thank you from the bottom of my heart.

I would like to specifically thank my parents, who have always encouraged the pursuit of my scientific interests. I was in the sixth grade when I completed my first project for the elementary school science fair. Unfortunately, no effort had been made by the school to provide me with the option of entering the county fair. It was my mother who called the director of the county science fair so that my project entitled “Building Bridges” was entered- it won an award. My father, ever the electrical engineer, taught me how to build a home-made light bulb when I was in the second grade. Throughout my collegiate studies I would often seek his advice regarding my work. His response, no matter the question, was always, “ $V = IR$ ”. He was right most of the time.

I would like to extend my thanks to Dr. Borovetz, who has been a great mentor to me since I was an undergraduate. His door was, and still is always open for professional advice, or witty jousts about who is the faster runner (I still think it’s me). To Dr. Antaki, for bringing me into his lab and sharing his abundance of knowledge, and unique approach to research and design; to the members of the Artificial Heart Program, from whom I have gained more experience than could ever be obtained from simply learning in the classroom; and to Dr. Bhama for assisting me with my experiments, his surgical talent made them a reality.

Finally, I would like to take this time to remember and thank the patients who I have met while working at the Artificial Heart Program. When working in the lab, it is easy at times to forget why we are doing this. Having the opportunity to work with those who receive these devices and watching them overcome great adversity has been a constant inspiration, and motivation to run that extra study, or stay that extra hour and review the results just one more time.

1.0 INTRODUCTION

1.1 CARDIAC FUNCTION, FAILURE, AND TREATMENT

1.1.1 Human Cardiac Physiology

Blood circulates in a closed loop through the body to exchange nutrients, oxygen, carbon dioxide, waste, and heat. It does this in 2 separate circuits that are connected in series: the systemic circulation and the pulmonary circulation. The pulmonary circulation passes through the lungs which function to oxygenate the blood. The systemic circulation delivers this oxygen rich blood to all other organs and muscles where the oxygen is consumed. The heart is the organ responsible for generating a difference in pressure that will generate the flow of blood. To maintain these circulations, the heart functions as a simultaneously contracting, pulsatile, double pump, separated by a septal wall into a right side to generate pulmonary circulation, and a left side to generate systemic circulation. Each side consists of two chambers: an atrium and a ventricle. The atria act as both passive conduits for venous return to the respective ventricles and also actively prime the ventricles with an additional volume of blood just prior to contraction of the ventricles. The ventricles are main pumping chambers that forcefully eject blood through blood vessels. From the left ventricle, blood is ejected into the main artery called the aorta. From the aorta, blood flows through arteries and arterioles and finally capillaries all over the body and is then collected again in veins that return the blood to the right atrium. The right ventricle then ejects the now deoxygenated blood through the lungs, after which ends up back on the left side of the heart. Since the systemic circulation consists of a multitude of tissue beds and encounters higher resistance, a higher pressure is required to maintain adequate perfusion. Mean aortic pressure in a healthy young person is about 120 mmHg to maintain a flow of 5.5 l/min. The right ventricle, in contrast, only has to generate a mean pulmonary artery pressure of about 10 mmHg

to maintain that same flow. Consequently, the left ventricle has larger muscle mass and is considered the main pumping chamber. It is also more prone to overloading and failure which may have consequences for multiple organs.

In order to maintain unidirectional flow, the connection between the atria and ventricles, and the connection between the ventricles and main arteries, are divided by valves. The pulmonic valve separates the right ventricle from the pulmonary artery, and the aortic valve separates the left ventricle from the aorta; the tricuspid valve separates the right atrium from the right ventricle and the mitral valve separates the left atrium from the left ventricle. Under normal physiologic conditions, the valves function to open only when the pressure within the proximal chambers exceeds that of the distal chamber or artery. Once the pressure in the distal chamber or artery exceeds the pressure within the proximal chamber, the valve closes. In order to provide additional mechanical support for the mitral and tricuspid valves, chordae anchor the valves to papillary muscles that contract during systole to prevent prolapse of the valve leaflets.

Throughout the cardiac cycle ventricles undergo a phasic motion of filling and ejecting, caused by muscle relaxation followed by contraction. One cardiac cycle consists of a systolic phase and a diastolic phase. The diastolic phase is the portion of the cardiac cycle when the cardiac muscle, or myocardium, relaxes. During diastole, the aortic and pulmonic valves are closed because the pressures in the right and left ventricles are less than the pressures in the pulmonary artery and aorta, respectively. This drop in pressure also opens the tricuspid and mitral valves, since the pressure within the ventricles drops below the pressure within the atria. During systole, the myocardium contracts, generating a rapid increase in pressure. The increase in pressure closes the mitral and tricuspid valves, and after a brief isovolumic contraction phase where both sets of valves are closed, opens the aortic and pulmonic valves.

The force with which the myocardium contracts is dependent on how much blood is in the ventricle at end-diastole, this end-diastolic volume is also referred to as pre-load. The greater the pre-load, the greater the force with which the heart contracts. This response is referred to as the Frank-Starling response. The heart must perform more work in order to contract harder; this increase in work also increases myocardial oxygen consumption. The change in volume from diastole to systole is called the stroke volume. Cardiac output, the product of stroke volume and heart rate, is controlled by the autonomic nervous system which can vary how rapid and how strong the heart beats in order to meet the demands of the body.

1.1.2 Heart Failure

Heart failure (HF) occurs when the heart is unable to adequately pump blood throughout the body. Inadequate perfusion of the tissues in the body can lead to multi organ system failure and eventually death. In congestive heart failure (CHF), the heart often becomes dilated from the backup of blood.

HF is one of the main causes of death in the United States. According to the American heart association, approximately 5 million Americans are currently suffering from HF. In 2005, nearly 1 million American men and women were discharged from hospitals with HF. The total cost of treatment for HF is over 34 billion dollars.[1]

Current medical therapy can treat CHF for some patients initially. However, over time the patient's heart will continue to deteriorate. The most successful treatment for CHF is a heart transplant. Unfortunately due to the large number of patients who could benefit from a transplant, and the short supply of donor hearts, many patients who are on the waiting list will die without ever receiving a heart. Ventricular assist devices (VADs) have emerged as a means of bridging a patient to transplant.

1.1.3 Ventricular Assist Devices

Ventricular Assist Devices (VADs) are blood pumps connected in parallel to the heart that assist the failing organ in maintaining sufficient blood flow and pressure. Since they take over part (or all) of the work of the failing ventricle, they can work as a stopgap until a donor heart is available, or otherwise said, as a bridge to transplant (BTT). A Left VAD (LVAD) is a pump that is connected most commonly to the LV apex by means of a cannula that is inserted through an incision in the myocardium. Blood in the LV drains through the cannula and is then pumped back into the ascending aorta where it travels throughout the vasculature. Unloading of the ventricle decreases ventricular preload and prevents the heart from contracting as hard, thereby decreasing the amount of work that it must do. Although most frequently used as a bridge to transplant, these devices can be used as destination therapy for patients who are not candidates for transplant, and will therefore be dependent on the device for life. Additionally, a subset of VAD patients has been able to recover enough native ventricular function to no longer need a

transplant. This bridge to recovery can prompt explantation of the device, while leaving the native heart in place.[2] [3]

First generation LVADs were pulsatile in an attempt to mimic the physiologic flow created by the beating heart. However, these implantable devices were large, and were limited to patients with large body surface areas, or were forced to be used extracorporeally. Second- and third-generation rotary pumps are designed to be smaller, allowing for a greater number of patients to be eligible for receiving a VAD. These rotary pumps are either axial or centrifugal, with a rotating impeller that actively draws blood from the ventricle and returns blood continuously to the aorta. Examples of both pulsatile and continuous flow pumps are shown in Figure 1. The output of first generation pumps depends mostly on patient preload; however, the output of rotary pumps depends on the preload, afterload and pump speed. This added complexity makes physiologic control of these pumps more difficult. An additional concern with rotary pumps is the collapse of the LV due to the negative pressures generated by the VAD.

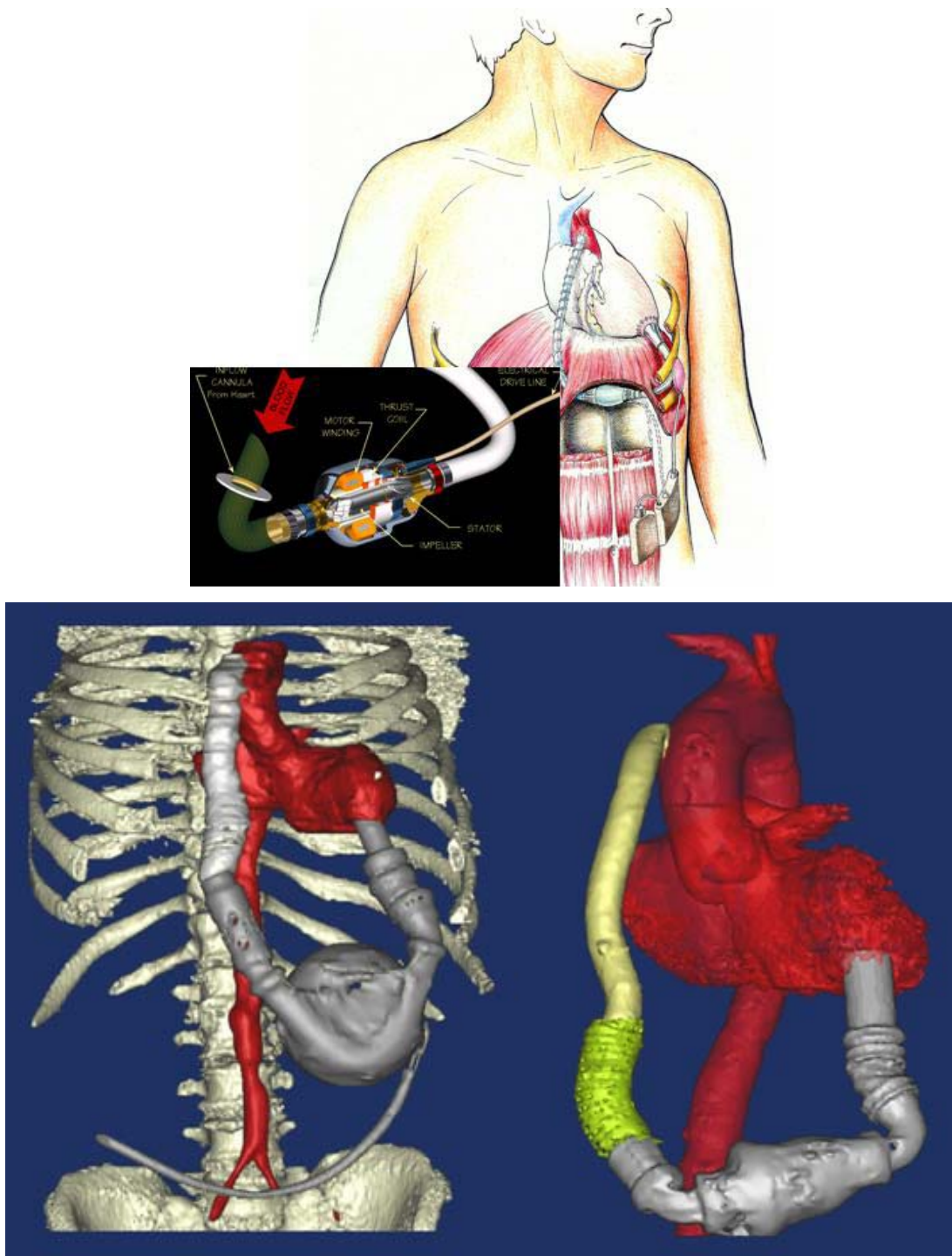


Figure 1-(Top) The Streamliner Axial Flow Ventricular Assist Device. (Bottom left) Reconstruction generated from a CT scan of a patient with a pulsatile HeartMate XVE LVAD. (Bottom Right) Reconstruction generated from a CT scan of a patient with an axial flow HeartMate II LVAD.

1.1.4 Current cannula options

Current cannula designs consist of straight tubing that extend into the chamber at varying depths. Some designs incorporate features at the end of the cannula tip to decrease the likelihood of obstruction by myocardium. Bevels, cages, and fenestrations are examples of these types of designs. Some LVAD inflow cannulae are designed to be placed in the left atrium; however it has been shown that ventricular cannulae are less likely to generate thrombus, and can sustain higher flows [4, 5]. Therefore it is more common to see chronic LVAD inflow cannulae that are designed to be inserted through the apex of the LV. Some examples of conventional cannula tip designs are shown in Figure 2.



Figure 2- Traditional inflow cannula tip geometries: (L-R) blunt, beveled, caged. The caged cannula is more commonly used for atrial cannulation.

1.1.5 Need for Improved Inflow Cannula

Extensive effort has been invested in optimizing the hemodynamics of turbodynamic ventricular assist devices. However, the hemodynamics of the ventricle-cannula interface remains a source of complication due to thrombosis, myocardial trauma, and obstruction. Most ventricular inflow cannulae are identical to- or simple modifications of- 1st generation cannulae. These cannula designs have been shown to cause adverse events that result in decreased pump outputs, and increased morbidity and mortality regardless of pump type (e.g. pulsatile or continuous). [6] The advent of turbodynamic pumps has brought with it the additional problem of ventricular suction. These actively filling, continuous flow pumps are capable of generating negative pressures within the ventricle which can induce the collapse of the chamber. [7, 8]

Current cannula designs show susceptibility to malpositioning and post-operative movement. Unfortunately, incorrect positioning may not become apparent until the chest of a patient has been closed and healed. A malpositioned cannula can lead to premature ventricular suction, entrapment of ventricular anatomy, activation of platelets or thrombus formation. Platelet activation and thrombus formation may not be apparent at the sight of the cannula. However, the activated blood must travel through further non-physiologic flow and can form emboli downstream. Prevention of ventricular suction and entrapment has been addressed via simple modifications of pre-existing cannulae by either adding vents or increasing the length of the cannula tip.[9] These remedies have actually increased the likelihood of thrombus formation due to jet formation resulting in high shear or increased exposure time of stagnant blood to raw myocardium at the apical wound site.

A recent study that evaluated numerous cannula designs during long-term use was presented by Kaufmann et al. at the 14th ISRBP- Congress in 2006. 10 different cannula types from 8 different pumps (3 pulsatile, 3 axial, 2 centrifugal) were evaluated based on post mortem examination or examination following transplant. Observations were made regarding how each cannula design contributes to thromboembolic events. It was concluded that an ideal cannula should have a textured outer surface to promote tissue integration, a smooth inner surface, a long tip protruding into the ventricle to prevent occlusion by cellular ingrowth, and a flexible and non-collapsible conduit leading to the inlet of the pump. The study however does not address how cannula design can assist in the prevention of malposition or collapse. [10]

In pre-clinical animal studies involving an axial flow pump, Snyder states that the vast majority of animals encountered adverse events. It was noted that a cannula with similar design to that described as desirable by Kaufmann caused septal scarring, frequent suction events, and entrainment of the septum. [11]

Though a common problem, few articles specifically address cannula positional sensitivity, many of which are limited to case reports, small patient numbers, or brief remarks. [12] [13] [14]

Ventricular suction causes a drop in flow that should not occur otherwise. This can be exacerbated by arrhythmias which can be generated by the event[15]. These arrhythmias can cause a further drop in flow. While improved controllers that are being developed can help prevent suction, [16-18] current designs do so by limiting the output of a pump, or simply do

nothing at all. A more robust cannula design can help alleviate a pump's sensitivity to mild suction conditions, thereby increasing physiologic range in which a pump can provide adequate flows to the patient.

1.2 PREVIOUS CANNULA DESIGN EFFORTS AT THE UNIVERSITY OF PITTSBURGH

The work in this thesis is part of an ongoing attempt to optimize the apical ventricular inflow cannula for ventricular assist devices. The design of the novel flared cannula, referred to as the “Quintessential Ventricular Cannula” (QVC), introduced in later chapters, is based on the initial findings of Dr. James F. Antaki, Ph.D.; and of Alison Curtis, M.S., whose work was performed under the advisement of Dr. Antaki. Their work, both published and unpublished, is presented in this section.

1.2.1 Antaki et al

In 1995, Antaki et al introduced a novel “trumpet mouth” cannula design, shown in Figure 3. The design addressed the problems that occur with inflow cannula of axial flow devices. Specifically, the design provided for greater stenting at the apex of the LV, proper placement during insertion, and avoidance of regions of flow stasis which could generate thrombus. This revolutionary cannula design was evaluated in acute and chronic in-vivo studies against a beveled, blunt, and caged tip cannula, similar to those in shown in Figure 2.

In the acute studies, hemodynamic performance was evaluated under various conditions. In addition to flow and pressure measurements, transepical echocardiography was used to visualize the flow characteristics for qualitative analysis. The traditional cannulae performed as well as the trumpet cannula under ideal, low-flow high-volume conditions. However, under low volume states, the trumpet cannula was able to achieve flows of up to 9 Lpm, while the traditional designs were only able to produce flows of 5-6 Lpm. In addition, the traditional cannulae were found to interfere with anatomic structures, creating areas of high shear.

Ambiguity of placement was also noted when attempting to determine the ideal depth of placement for the beveled, caged, and blunt geometries.

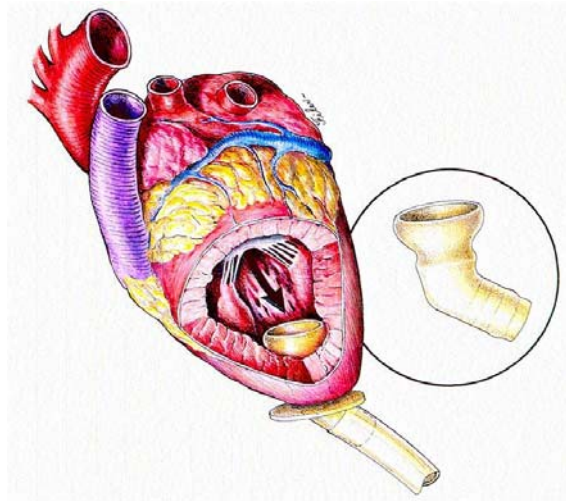


Figure 3-Trumpet mouth cannula tip introduced by Antaki et al

Chronic in-vivo studies were performed for a period of 28 days. Post mortem examination found irritation of the myocardium for all three conventional geometries, while minimal irritation was noted for the trumpet design. The examination also found that the conventional geometries were prone to thrombus formation. Figure 4 shows the resulting post mortem photos of the various cannula types, including a spherical thrombus formed at the tip of the caged cannula and a beveled cannula that has entrained a portion of the papillary muscle with a large apical thrombus formed due to flow stasis.

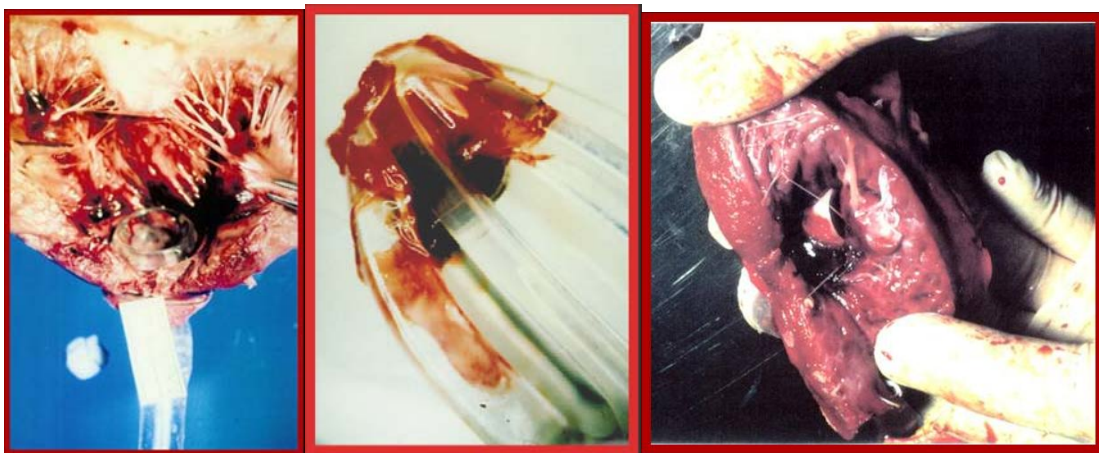


Figure 4-(Left) Dissected LV with trumpet cannula. (Middle) Thrombus produced by blood flow at tip of cage. (Right) A malpositioned cannula with entrained papillary muscle. And large thrombus formed at the apex, where blood has stagnated.

The trumpet cannula while far more ideal than conventional cannula did have its shortcomings. Due to the rigid material used, and the large diameter of the wide mouth with respect to the small diameter of the neck, surgical implantation of the cannula was found to be difficult. [19]

1.2.2 Curtis et al

Curtis et al performed in-vitro flow visualization testing to validate the in-vivo findings of Antaki et al. Fluorescent particles were illuminated in transparent mock ventricles, fabricated from casts of contracted and relaxed bovine ventricles. The contracted LV molds were tested with steady flow, while a valve was placed at the proximal end of the dilated LV molds, which were pressurized in and depressurized in order to simulate ventricular wall motion (see Figure 5).

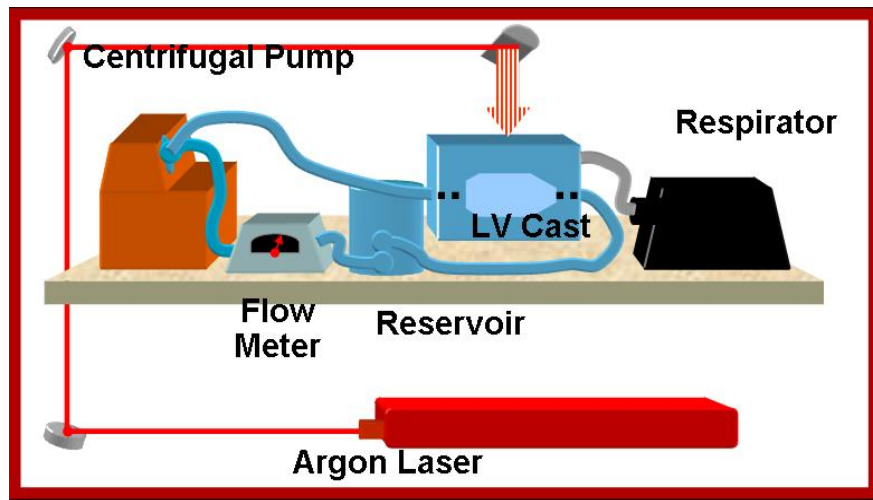


Figure 5- In-vitro setup used for visualizing the flow within the cannulated ventricle casts

The findings of Curtis et al. agreed with those of Antaki et al. The flow visualization generated images that illustrated exactly what was believed to have occurred in-vivo. Figure 6 illustrates the regions of stagnation or recirculation of particles. The cannulae with openings protruding well into the ventricle generated significant areas of stagnation near the apex, and the caged cannula formed a region of stagnation in the same region that thrombus was found following post mortem inspection in 1995. There was no region of stagnant flow found with the trumpet mouth. The flow appeared laminar within the steady flow experiments and displayed good washing with pulsatility. [20]

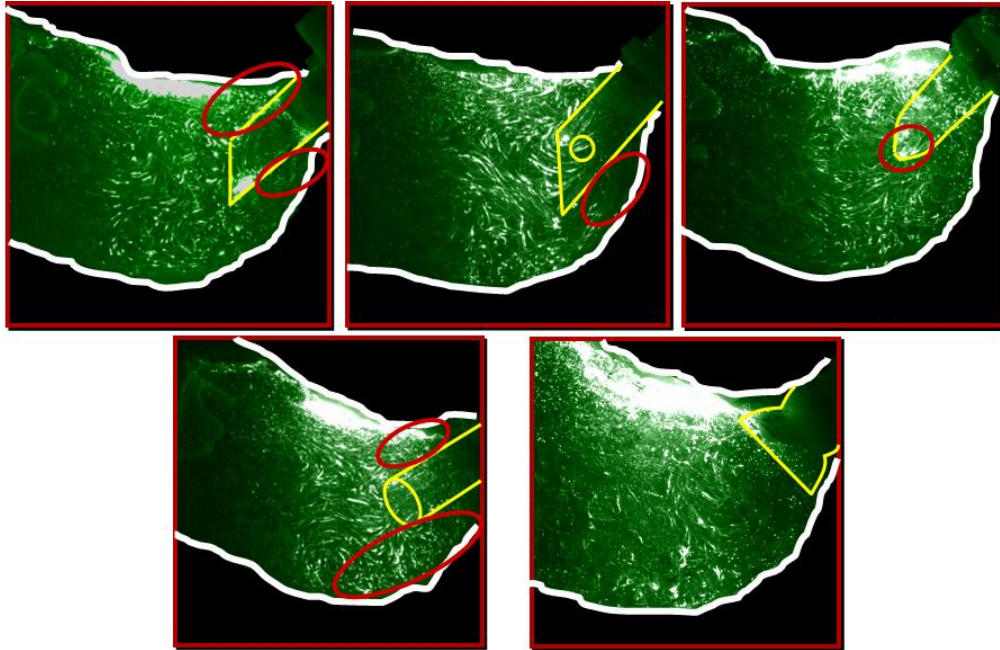


Figure 6-Flow visualization of performed by Curtis et al. using various cannula geometries in transparent bovine LV casts: (Top left) beveled; (Top middle) beveled with side vent; (Top right) caged; (Bottom left) blunt; (bottom right) trumpet tip. The red circles indicate areas of stagnation or recirculation; the yellow and white lines are intended to help clarify the boundaries of the cannula and ventricle wall respectively. (Note: the large bright spots at the top of each ventricle are from the laser reflecting off of the wall, and should not be interpreted as collecting particles)

2.0 CANNULA DEVELOPMENT

2.1 DESIRED CANNULA FEATURES

2.1.1 Attachment

An ideal cannula design is one that facilitates a fast and uncomplicated pump implantation. It must provide for easy and rapid insertion in a consistent manner. In order for the insertion procedure to be as short as possible, there can be only a few, easily repeatable steps. Simple tools such as a coring device and introducer limit the variability that can occur from surgeon to surgeon, while simultaneously expediting the procedure. The Cannula properties itself must help to reduce the likelihood of variability during insertion by guaranteeing proper positioning every time. Also, because the VAD is capable of shifting while the heart is lowered back into the patient, the cannula design must eliminate positional sensitivity due to changes in orientation.

2.1.2 Geometry

2.1.2.1 Hemodynamics

The ability of a VAD to adequately unload the LV is highly dependent on the ability of the cannula to drain blood from the LV and supply it to the pump with the least possible resistance, while reducing conditions that promote hemolysis and thrombosis. In order to produce hemodynamically favorable flows, the cannula tip must avoid creating areas of stagnation at the apex of the LV and from generating separation zones within the cannula.

2.1.2.2 Anatomic Fit

The geometry of the cannula should be one that minimizes interference with the anatomic features found within the chamber of the LV. This includes the mitral apparatus and trabeculae. In patients who are hypovolemic, the cannula geometry must minimize occlusion due to ventricular suction. This geometry must also prevent premature ventricular suction due to post operative cannula shift. Finally, the cannula geometry must minimize the exposure of raw myocardium, generated by the cannulation procedure, to blood, which could possibly generate thrombus.

2.1.3 Materials

2.1.3.1 Mechanical Properties

The materials used to fabricate the cannula must be strong in order to maintain the cannula's shape; but not too rigid, in order to allow for adjustment to various ventricular geometries. The cannula must be able to withstand forces exerted upon it by the contracting heart, by the myocardial wall at negative pressures, and must also be able to recover its shape after cross-clamping during surgery.

2.1.3.2 Biocompatibility

A major concern for any chronic blood contacting device is biocompatibility. The internal surface of the cannula tip and conduit must avoid the generation of thrombus which could impair pump flow, or cause a stroke. The external surface of the cannula, especially that which comes in contact with the myocardium must not irritate the surrounding tissue. In addition, the international Standards Organization (ISO) has released a document ISO 10991-2. This document summarizes the biocompatibility requirements for any acute, short term, or long term blood contacting device. In addition to the biocompatibility requirements stated above, ISO standards require that a blood contacting device that is implanted for greater than 30 days will not cause any adverse biological effects due to cytotoxicity, sensitization, systemic toxicity, genotoxicity, chronic toxicity or carcinogenicity.

2.2 QVC CANNULA

A team consisting of engineers from the University of Pittsburgh, Carnegie Mellon University, and LaunchPoint Technologies, LLC developed a novel cannula based on the findings of Antaki and Curtis, and the requirements in section 2.1. The resulting design was the novel, monolithic QVC, possessing an internal flare that fits the form of the endocardial wall, and an external clasp that applies pressure to the pericardium, to ensure that the internal flare stays flush to the surface. In addition, ribs were added to the external surface of the conduit portion of the cannula, in order to provide reinforcement of the cannula, to prevent kinking or permanent deformation after being cross-clamped. Figure 7 shows variations of the QVC along with a cross-sectional view of the final design.

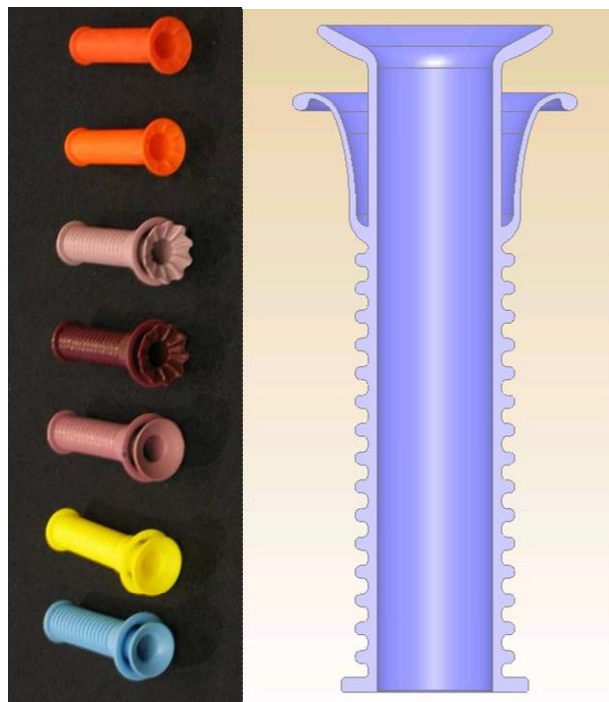


Figure 7- (left) Iterations of the QVC. (Right)Section view of final flared design

The material used to fabricate the cannula was a pre-existing polymer made by BJB Enterprises (Tustin, CA). Actual Manufacturing was performed by Spectrum 3D, Inc. (Tustin, CA) This material possesses great flexibility while maintaining a high memory. These qualities allow the internal flare to be compressed, as shown in Figure 8. The ease in which the flare can be manipulated allows it to be easily deployed through holes of smaller diameter than the

internal flare (in this case the diameter that the cannula must pass through is the diameter of the ventricle core that has been cut from the myocardium.) Figure 9 illustrates the ability of the Flare to be deployed through holes of a smaller diameter



Figure 8- The high memory polymer used to fabricate the QVC allowed it to be folded and compressed in order to facilitate easy insertion into the LV



Figure 9- the QVC deployed through a piece of acrylic. The diameter of the flare, far exceeds the diameter through which it has been inserted

3.0 CANNULA EVALUATION

3.1 ANATOMIC FIT STUDIES

3.1.1 In-silico

One of the key steps in determining how to design an optimal cannula is to gain an understanding of the cannula's surroundings, and how those surroundings interact with the cannula. For an apical cannula placed in a left ventricle, it is incredibly important to understand the internal anatomy of that chamber. A sub-optimally designed, improperly placed cannula can increase the chances of interference of the mitral apparatus or the ventricle wall. These interferences can obstruct the inflow tract of the cannula, severely impairing the cannula's ability to facilitate adequate drainage for the pump.

Previous studies of ventricular anatomy performed by this lab have used human cadaver, bovine, goat, and porcine hearts to create molds of the LV. These molds were either rigid or semi-rigid, and were used as a reference tool as well as for flow visualization. These methods, however, have many shortcomings. Human cadaver hearts provide only limited information to the investigator. The heart is no longer beating, and it can change shape after being manipulated. Animal hearts often have ventricular wall thicknesses that are much greater than that of a human, in addition to having geometries that vary depending on the species.

A better method was needed to understand the ventricle's geometry, in-vivo and undisturbed. Electronic, three-dimensional anatomic reconstruction presented itself as a means for obtaining morphometric data of a human ventricle in its various geometric states throughout the cardiac cycle.

The reconstructions, made from ECG-gated CT images made it possible to study the anatomy electronically, to design the cannula, to determine proper placement. And although not

discussed in detail in this thesis, these reconstructions can be used to design elements that would later be manufactured for in-vitro validation of the cannula.

3.1.1.1 Methods

Prior to the acquisition of patient data and images, University of Pittsburgh Institutional Review Board approval was received. After approval was granted, de-identified patient data were obtained via honest broker from the University of Pittsburgh Medical Center Presbyterian Hospital Department of Radiology. Patient data included CT scans of the heart at end systole and end diastole, the patient's diagnosis, age, weight, and gender.

ECG- gated CT scans were chosen for their availability, high resolution, and ability to determine stage of cardiac cycle. Patient conditions chosen reflected those commonly requiring mechanical circulatory support.

CT images were received as Digital Imaging and Communications in Medicine (DICOM) files, which store both image and positional information. The DICOM files were imported into Mimics 3D imaging software (Materialise, Ann Arbor, MI). Upon importing into Mimics, the actual reconstruction process began.

In Mimics, the CT images are re-sliced and the contrast is adjusted so that the best view possible of the area of interest is displayed. Figure 10 shows the initial CT scan, adjusted contrast and direction of reslicing. Thresholding is then performed, highlighting the area to be reconstructed. For the reconstructions, the blood occupied volume (enhanced by a contrast agent during the procedure) was selected. Thresholding generates a mask for each CT scan slice. Manual editing of the initial masks removes artifacts that are unnecessarily highlighted to leave only the region of interest for generation of the 3D endocardial surface. Figure 11, Figure 12, and Figure 13 illustrates the generation of an initial mask and the refinement of the reconstructions using manual editing techniques.

At this point in the process the reconstructed surface is still rough. Also, in its current state the geometry can only be viewed in software developed by Materialise. In order to smooth the surface and generate a data format that can be read by conventional CAD software, the surface data is exported from Mimics as a point cloud. This point cloud (shown in Figure 14) is then imported into Raindrop Geomags Studio 8 (Geomags), a reverse engineering software program that specializes in the generation of CAD surfaces. Within Geomags, the point cloud

is converted into a polygonal surface that consists of thousands of small triangles. This polygonal surface closely resembles the manually edited surface that was originally made in Mimics. The new surface can be made water-tight and then smoothed (Figure 15 and Figure 16). From there, patches can be drawn along the contours of the surface and grids are fit within each patch. Finally, the geometry is converted into a CAD surface that can be exported as a common CAD file (Figure 17).

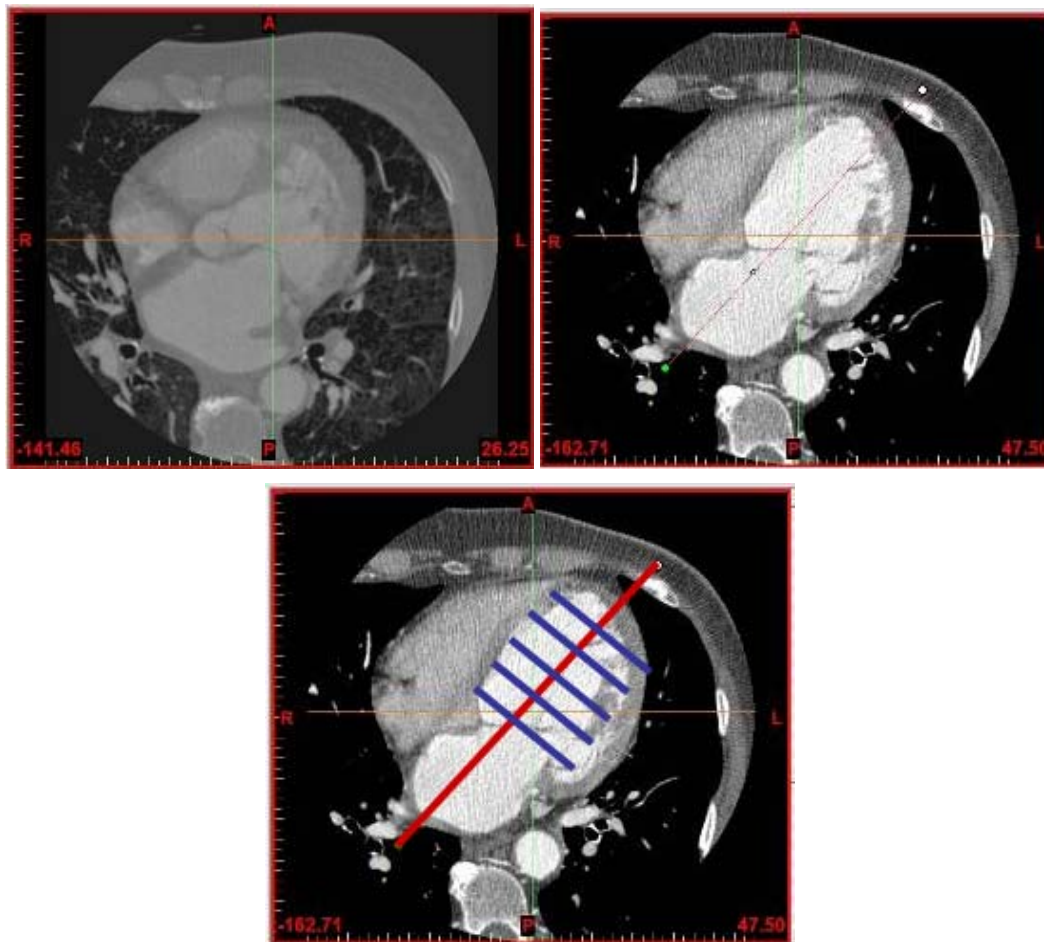


Figure 10- (Top Left) Initial CT scan of chest, imported into Mimics. (Top Right) CT scan with enhanced contrast. (Bottom) Image was resliced along long axis (red line) in order to obtain short axis view of LV

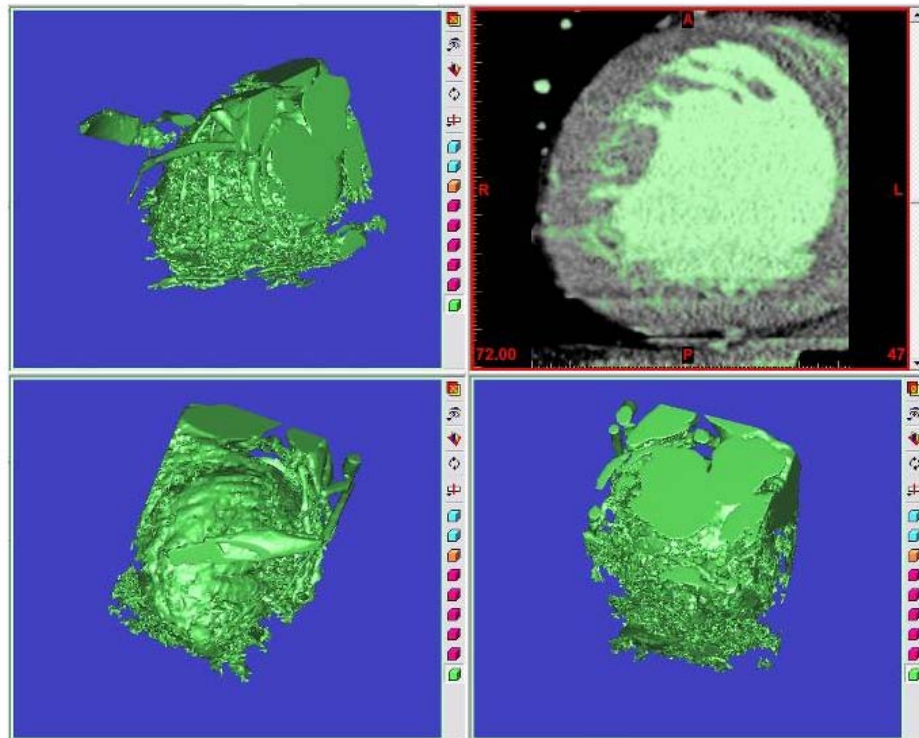


Figure 11- Segmented LV

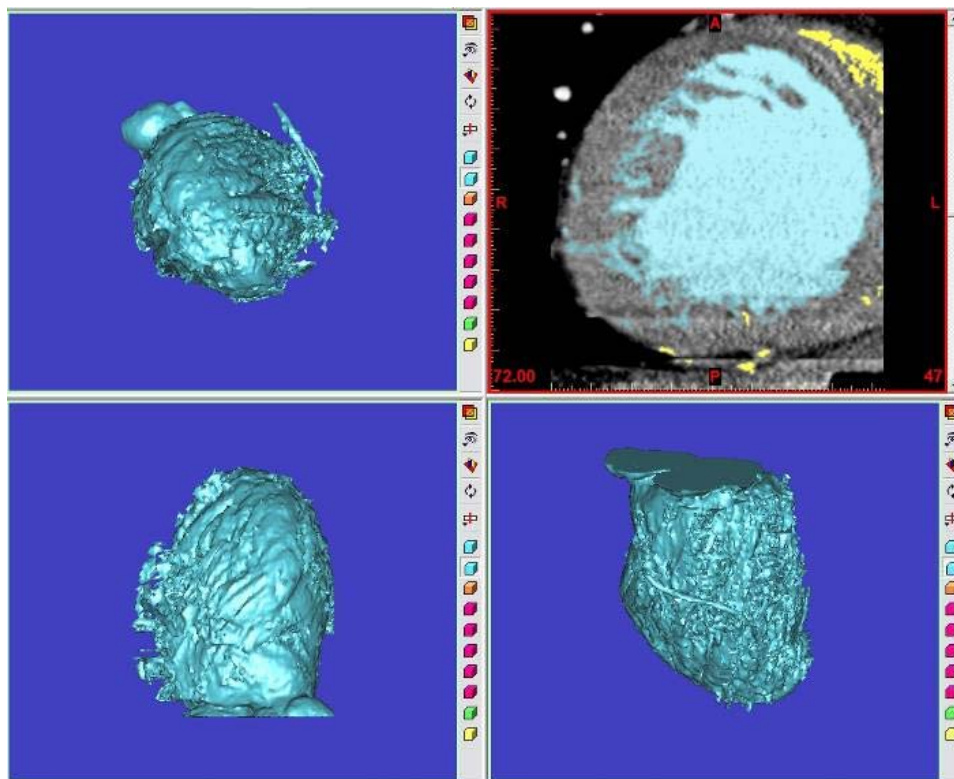


Figure 12- removal of artifacts

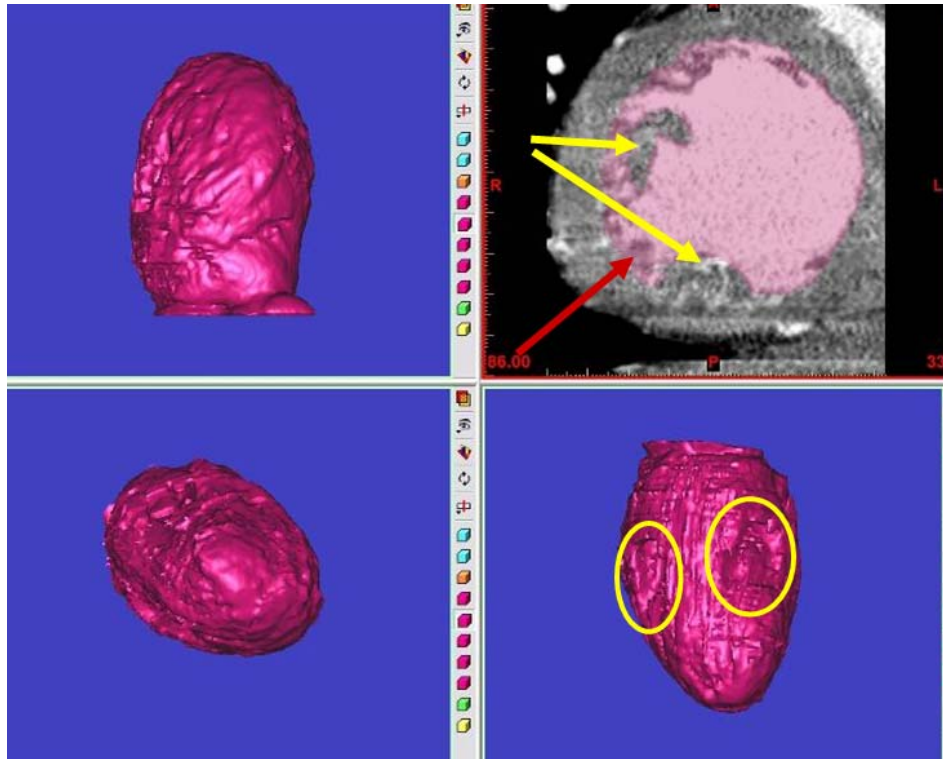


Figure 13- Manual editing of reconstruction in Mimics. The yellow arrows indicate the papillary muscles and the yellow circles indicate the resulting undercuts in the reconstructed blood-occupied volume. The red arrow shows where detail such as trabeculae have been omitted in order to reduce noise.

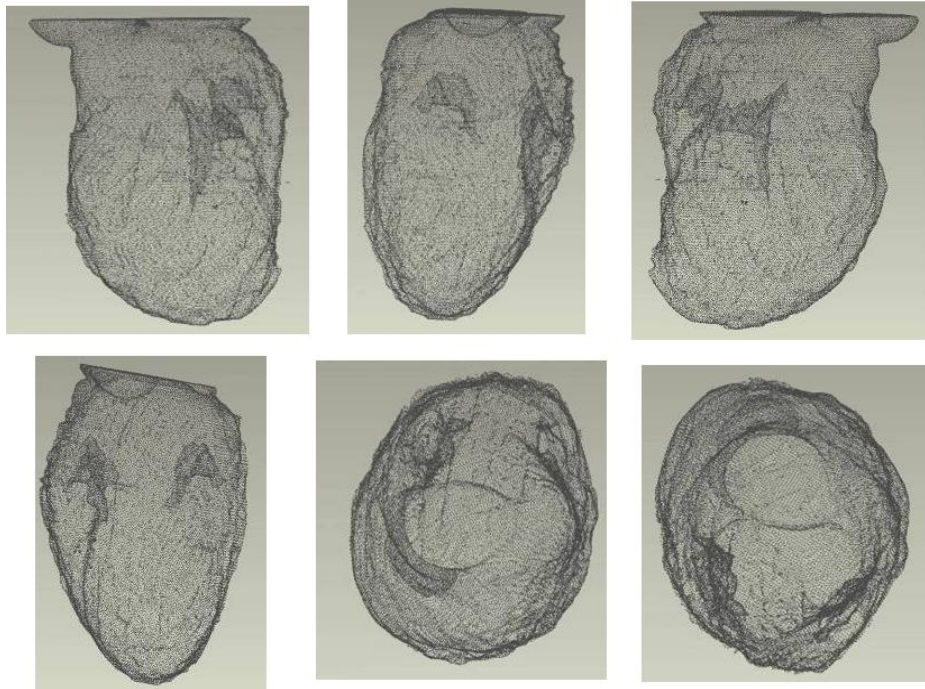


Figure 14- Point cloud imported from Mimics into Geomagics

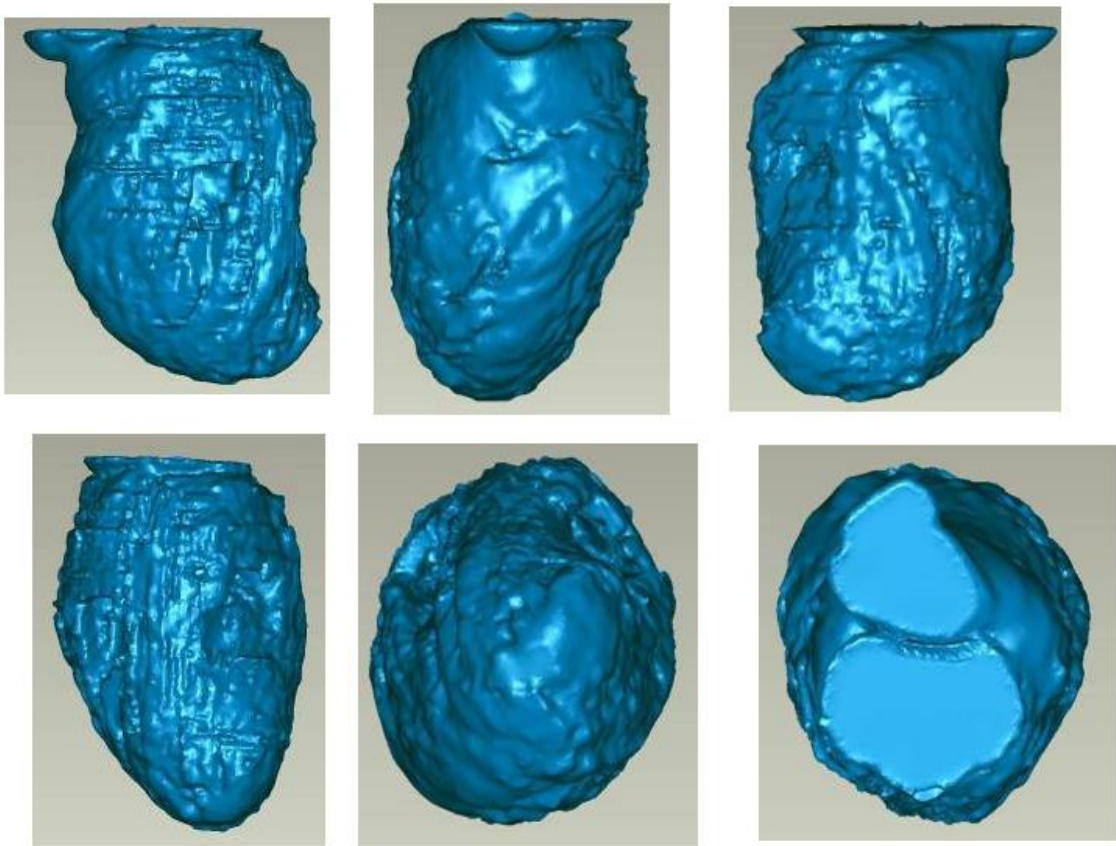


Figure 15-Polygonal surface

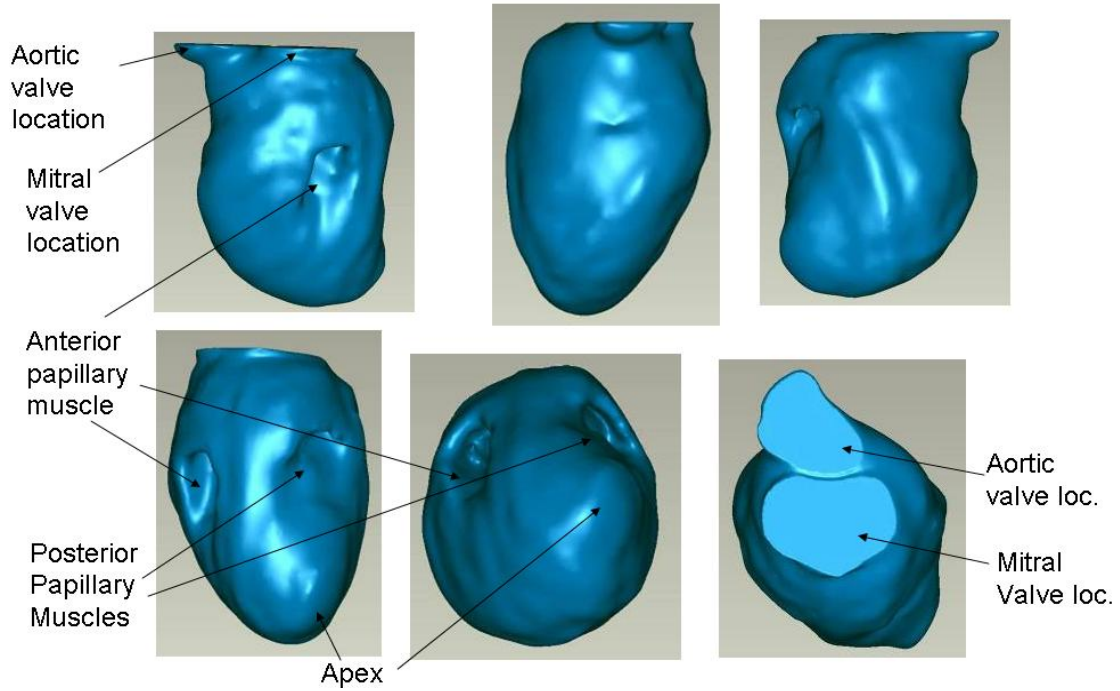


Figure 16- Polygonal surface following noise reduction

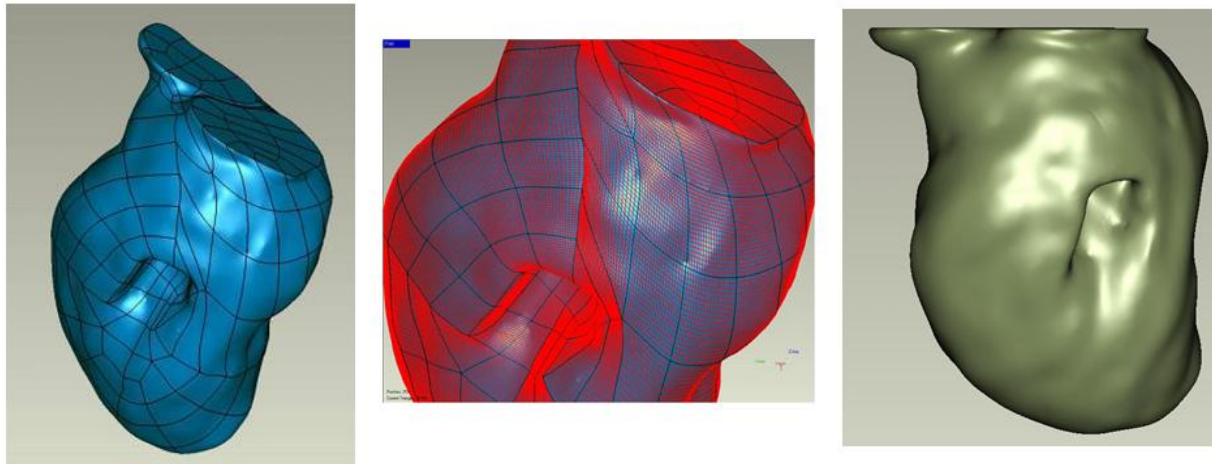


Figure 17-(Left) Grid generated on surface. (Middle) Mesh fit within grid. (Right) Resulting Surface than can be exported to CAD programs

3.1.1.2 Results

Figure 18 shows the resulting reconstructed ventricles at end systole and end diastole. End diastolic volume was calculated as 320.7 cc, and end-systolic volume is 249 cc. The

reconstructed ventricle has a calculated ejection fraction of 22.4%. It should be noted that these calculations are only approximate, because the volumes include the mitral and aortic artifacts.

Figure 19 shows the resulting changes in surface topology, and that the largest height change due to addition or subtraction of material for a reconstructed ventricle is approximately 2.6mm. Since the ventricles being generated are meant to be idealized, the accuracy of the ventricle appears reasonable for its intended purpose.

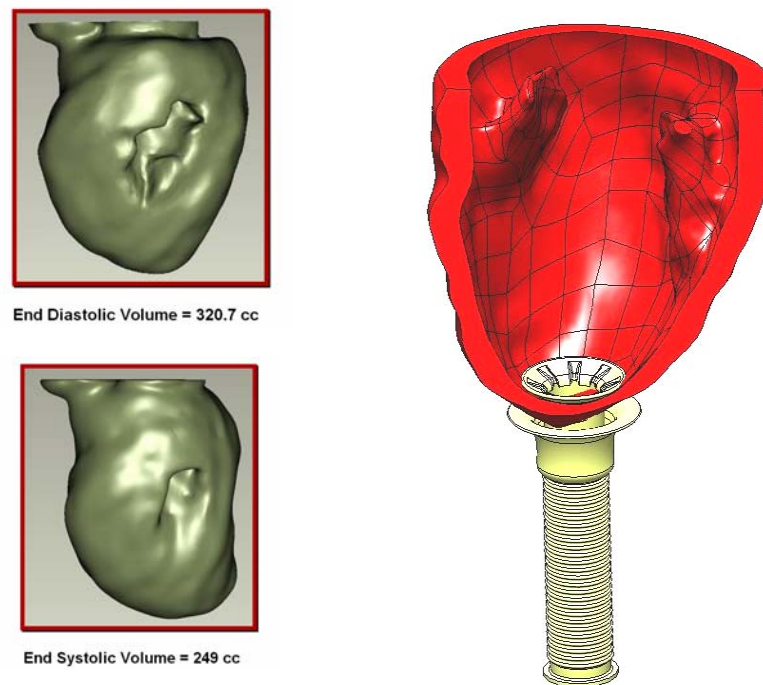


Figure 18- (Top Left) CAD surface at end-diastole. (Bottom Left) CAD surface at end-systole. (Right) Usage of the CAD surface to analyze the interaction of the QVC with the LV anatomy

3.1.1.3 Discussion

The reconstruction process often requires subjective interpretations of the anatomy. It is sometimes difficult for the reconstruction software to know the difference between actual anatomic structures and noise. Manual editing can compensate for this; however, it raises the question of reconstruction accuracy. While Mimics does not possess the ability to measure the amount of any reconstruction that is removed from one step to the next, Geomagics does have the ability to measure how much material has been added or removed by the noise reduction process.

While it is apparent that the reconstructed “idealized” heart closely resembles that of the actual heart, limitations of the technology used prevent such structures such as chordae and trabeculae from being included. The resolution of the available CT scans was not sufficient to differentiate noise from detailed anatomy. Such small detail is not pertinent for determining whether the cannula fits properly, as the cannula will press itself flush against the wall, and upon examination after coring, a surgeon can remove nonessential anatomic features.

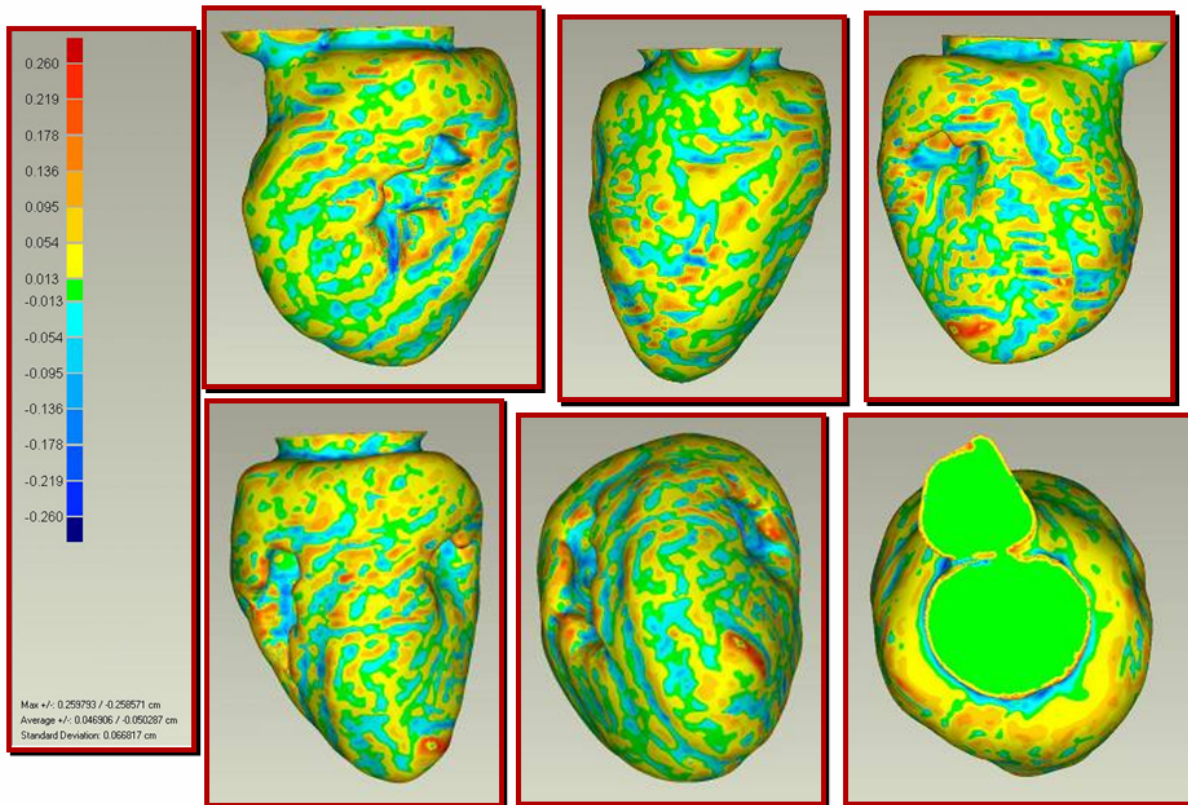


Figure 19- Changes in elevation generated during end diastolic surface noise reduction.

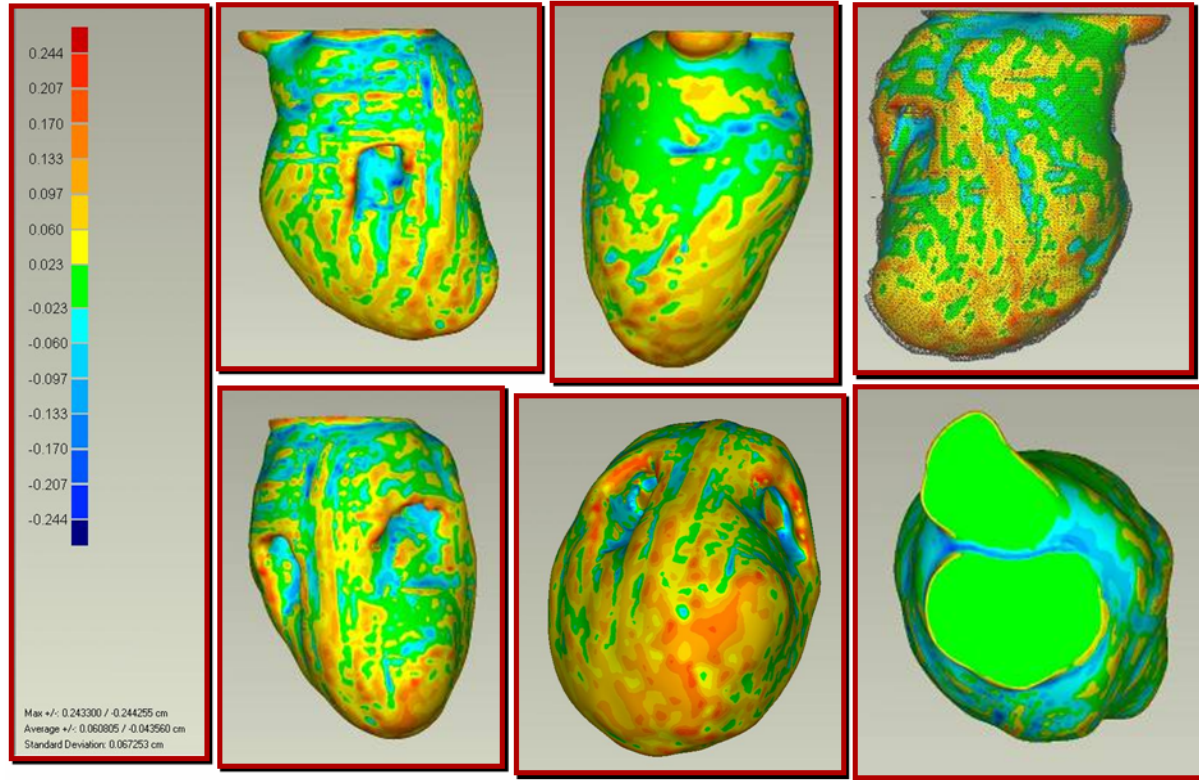


Figure 20- Changes in elevation generated during end systolic surface noise reduction.

3.1.2 Ex-vivo

Following multiple design iterations, and electronic evaluation of anatomic fit, the final cannula designs were fabricated and tested in several bench-top tests in order to validate what was determined in-silico.

3.1.2.1 Methods

A heart from a deceased 50 kg goat was cored at the LV apex, and the QVC was inserted. The left atrium and basal lateral, posterior and anterior portion of the left ventricle of the heart were dissected, exposing the mid-level and apical regions of the ventricular wall. The septum was left intact. The cannula was exposed and qualitative observations were made regarding the anatomic fit at both ideal and malpositioned conformations. The QVC was then removed and a vented, beveled cannula geometry was inserted. Observations were also made for the beveled cannula.

3.1.2.2 Results

The QVC showed a flush fit against the myocardium. There was no interference with the papillary muscle or chordae. When torqued, the QVC remained flush against the wall, even when bent at a severe angle. The conventional cannula, even when properly placed, generated large crevices between the orifice of the cannula and the apical wall. The cannula was easily malpositioned. When torqued only slightly, the cannula quickly came in contact with the lateral wall, due to the extended length.

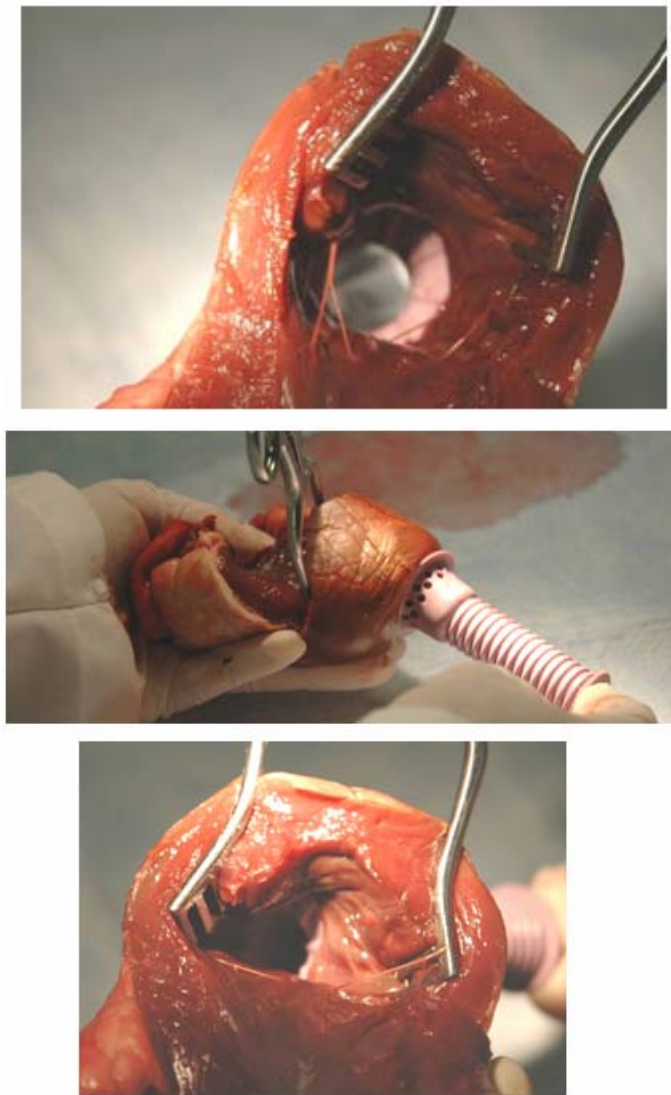


Figure 21-(top) properly placed QVC design. (Middle) external view of torqued cannula. (Bottom) internal view of torqued cannula.

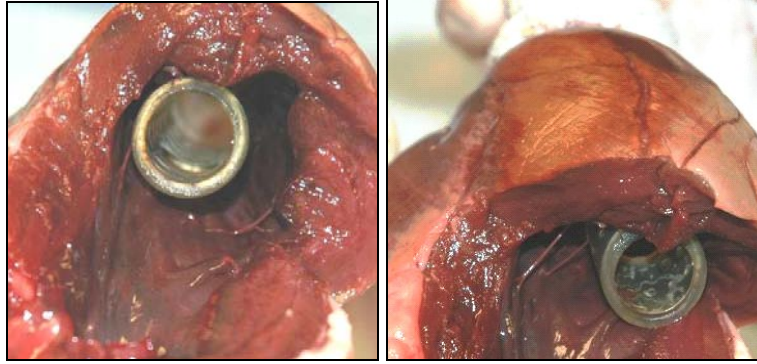


Figure 22-(Left) nominally placed beveled cannula. (Right) Slightly torqued beveled cannula now pointed towards ventricular wall.

3.2 CANNULA PULLOUT STUDY

3.2.1 Description of study

A test was developed and completed that examined how much force is required to remove the QVC design from myocardial tissue. Cannulated sections of bovine myocardium were supported by a frame that was hung from a load cell. Water was poured into a container attached to the cannula, which would in turn be gradually pulled from the tissue sample. The load applied to the cannula was recorded in real time and was used to indicate the maximum load applied. Samples were each cut from separate hearts. The maximum forces withstood by the cannula, when placed in samples, cut from hearts weighing 1844 g, 2157 g, and 2086 g, were 17.41 N, 18.96 N, and 16.77 N respectively. A significant amount of force is needed to pull the non-sutured cannula from the cored samples; however, more tests need to be run in order to perform further analysis.

3.2.2 Methods

3.2.2.1 Preparation of myocardium

Mature bovine hearts were acquired from a local slaughter house (Thoma's Meat Market, Saxonburg, PA). The mass of the heart was recorded. The right ventricular (RV) myocardium was cut away from the left ventricle and laid flat on the table top. The chordae tendonae were

cut away from the papillary muscle and the tricuspid valve was folded back from the endocardial surface. A 3.5 in x 3.5 in square pattern, with a circular hole in the center, was placed on top of the RV. The pattern was then cut out using a scalpel, and a custom made coring tool was used to make a circular cut through the myocardium. The core size was 2mm less in diameter than that of the cannula shaft to be placed in it. This was done to assure a tight fit.

3.2.2.2 Supporting the myocardium and placement of cannula

A custom made acrylic frame was designed in order to hold the myocardium in place during the experiment as well as to transfer the force exerted on the cannula to the load cell. The frame, made from acrylic, possessed four holes which allowed skewers to be placed through the myocardium in an overlapping crisscross fashion. The frame was designed to then be hung on a load cell after strings were attached to the hooks at each corner. The section of myocardium was then placed within the frame. Four skewers were inserted through the length and height of the section. Finally, a QVC with external flange was inserted by folding the cannula tip into an “S” conformation and placing it through the sample. Once through, the cannula was allowed to expand completely. Figure 23 shows a top and bottom view of the cannulated section.

3.2.2.3 Force application, measurement, and data acquisition

In order to place a constantly increasing force on the cannula, a Biomedicus Pump was used to pump water into a container that was hung from the cannula being tested. The force applied to the cannula was measured using a Wagner Force Five FDV-10 load cell (Wagner Instruments, Greenwich CT). The load cell was connected to an Iotech TB-100 data acquisition (DAQ) board (Iotech Inc., Cleveland, OH). Labview software was used to read the signal from the DAQ board. Figure 24 shows the final experimental setup.

3.2.2.4 Experimental Procedure

The frame supporting the cannulated myocardium was hung from the load cell and a fluid container was hung from the cannula. The Biomedicus pump (Biomedicus, Minneapolis MN) with a Medtronic Bio-Pump BPX-80 pump head (Medtronic, Minneapolis MN) was clamped off and set to a speed of 2000 RPM. The DAQ software was set to a sampling frequency of 200 Hz and was started. Upon commencement of data logging, the outflow tube from the Biomedicus

Pump was placed in the container and was unclamped. The container was allowed to fill until the cannula had been completely pulled from the myocardium, after which time the test was terminated. The force data were plotted versus time in Microsoft Excel.

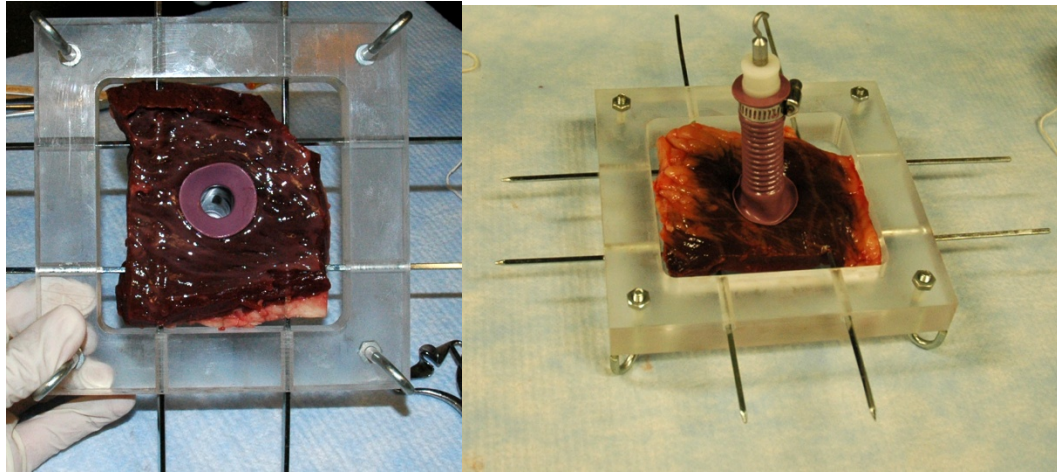


Figure 23- (Left) top view of supported and cannulated section. (Right) bottom view of same section.

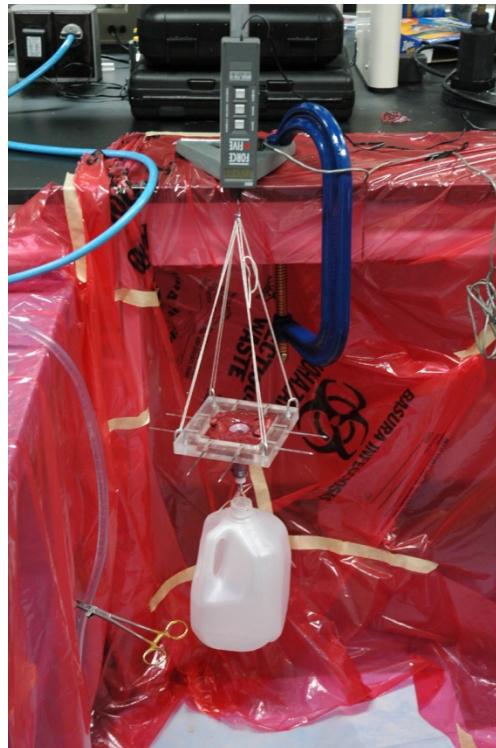


Figure 24- The test setup consists of a container hung from a cannula, attached to a supported section of myocardium, which transfers the force applied to the cannula to the load cell.

3.2.3 Results

Three tests were run; one test per sample. Each sample was cut from a separate bovine RV. The Bovine hearts weighed 1844 g, 2157 g, and 2086 g (it should be noted that the atria had been removed prior to acquiring the hearts). Figure 25 shows that the force applied by the water was increasing at the same rate for each run. The maximum forces withstood by the cannula, when placed in the samples from the hearts weighing 1844 g, 2157 g, and 2086 g were 17.41 N, 18.96 N, and 16.77 N respectively.

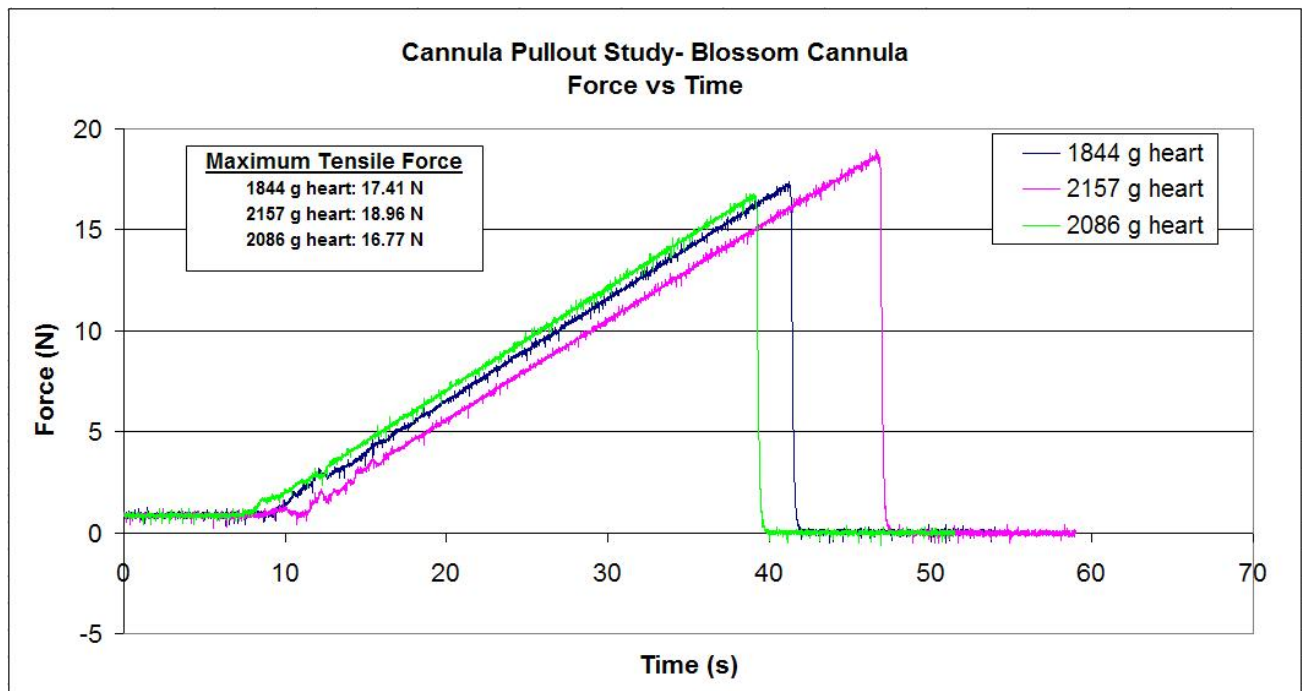


Figure 25- This graph illustrates that the force was increased at the same constant rate for each test. The peak and sudden drop in force also indicates the maximum force immediately prior to being pulled from the myocardium. Force does not equal zero at time zero, because the water container was hung from the cannula prior to commencement of data logging.

3.3 VENTRICULAR SUCTION STUDY

3.3.1 Description of study

An arrested isolated heart preparation was configured to enable borescopic visualization of the apically cannulated left ventricle in order to systematically investigate the influence of ventricular cannula position and design on ventricular suction. A conventional centrifugal pump was used to simulate the function of the LVAD.

The study consisted of two potential scenarios which cause suction events and are clinically feasible. The first condition that was simulated was hypovolemia. Suction often occurs when a patient has been experiencing post-operative bleeding or has been dehydrated. The second condition which causes suction is when the pump speed has been set too high in an attempt to completely unload the LV. During each scenario, the cannulae were tested at both nominal and suboptimal conformations.

Performance of a conventional beveled cannula, and the novel flared design was evaluated quantitatively by measuring the resulting flows produced by the pump and calculating the relative change in flow between nominal and suboptimal positions for each design. Qualitative analysis was performed via observation of flow fields and interaction between cannula and endocardial surface.

3.3.2 Methods

3.3.2.1 Experimental setup

Fresh ovine hearts were donated by a slaughterhouse (Zrile Meat Market, West Middlesex, PA). The ovine were approximately 8-10 months old at time of slaughter. Hearts were removed with pericardial sac and great vessels intact and were kept frozen until used in experiment.

After thawing, the pericardial sac was removed to allow access to myocardium, and the dome of the left atrium (LA) was dissected. A modified t-tube connector was inserted through the remaining left atrium and mitral valve. A purse-string was tied around the LA and small-diameter tubing was utilized to create a tourniquet which held t-tube in place. All remaining

vessels in the left heart, excluding the aorta, were tied off ensuring that the LV and remaining LA were water-tight. Figure 27 and Figure 28 illustrate the steps taken during heart preparation prior to and following cannulation. The prepped heart was connected to the flow loop. Intravenous tubing was inserted into the aorta and then clamped, allowing the aorta to be used as a vent for de-airing. A 30° borescope, connected to a CCD camera (Sony, model PV-420DN), was fed through the t-tube connector, beyond the mitral annulus, and into the LV. The shaft of the scope was oriented such that the field of view included the cannula and surrounding apical region of the endocardial surface. The apex of the LV was cored using a number 11 blade, allowing the cannula of choice to be inserted and attached as it would be in a human heart during surgery. Any non-essential anatomic features (i.e. tertiary chordae) of the LV were removed if found to interfere with the camera's view. The ventricular cannula was then connected to the inflow of a Biomedicus centrifugal pump. The centrifugal pump, which acted as the LVAD, returned the fluid to the reservoir. The reservoir was placed on a platform that allowed for height adjustment in order to adjust pre-load. In order to maintain a constant water level in the reservoir, a spill-over funnel was placed inside the reservoir. Any accumulation of excess fluid that would otherwise alter the pre-load spills over into the funnel and is returned through a secondary loop connected to a roller pump. The loop was primed with distilled water at room temperature, seeded with particles of Amberlite IRA-96 for flow visualization. As the heart was pressurized, the aortic vent was opened intermittently in order to allow air bubbles to escape.

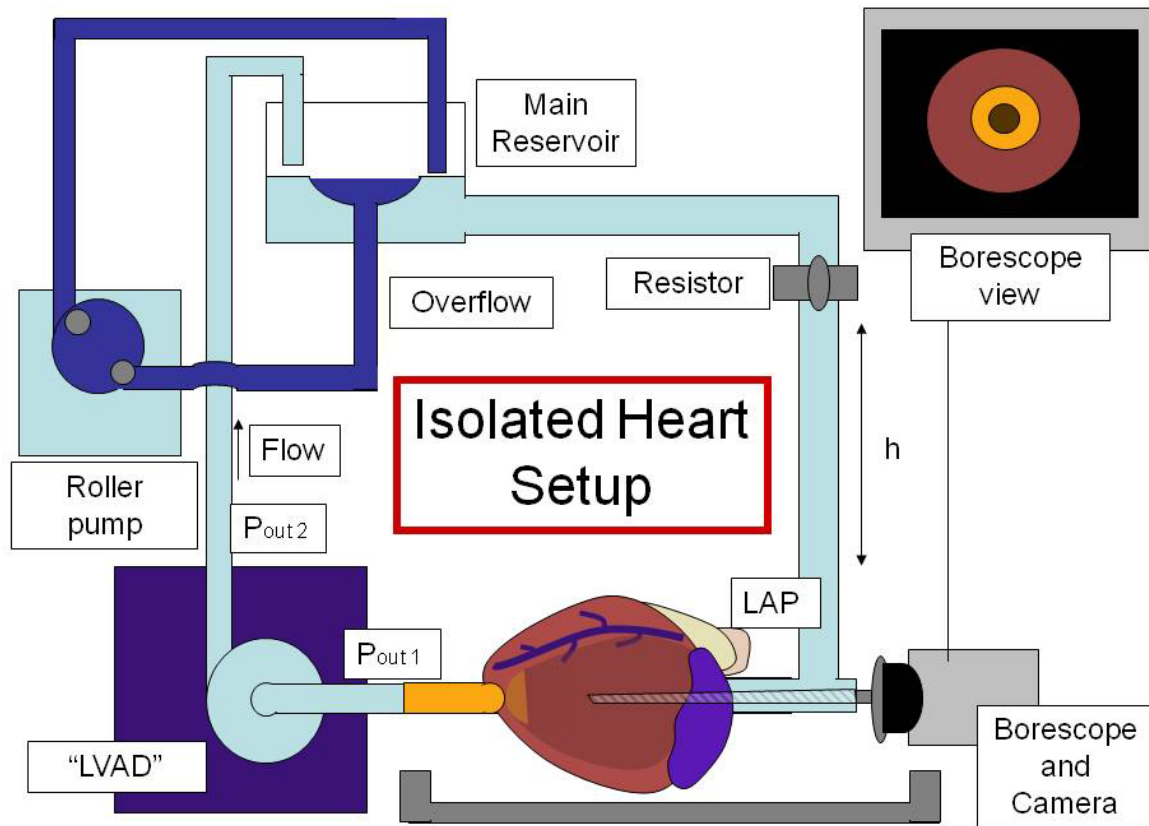


Figure 26- Diagram of suction setup



Figure 27-Ovine Heart Preparation: (Top-Left) Pericardial sac removed; (Bottom-Left) Left atrium dissected; (Middle) T-tube inserted and tied with purse string; (Right) drawing of the components that were assembled to create a leak-proof t-tube connector.

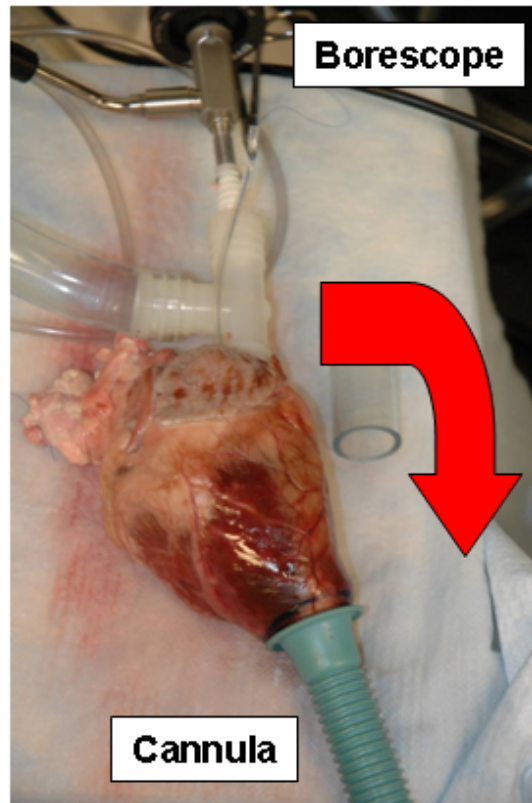


Figure 28-Loop setup showing borescope, cannulated LV, and direction of flow (indicated by arrow).

3.3.2.2 Experimental procedure

The experiment was performed using two different cannula designs: a conventional beveled cannula design and the QVC design with an internal tip diameter of 13mm and 14mm, respectively (shown in Figure 29). Both cannulae were tested when properly placed and when malpositioned. Malpositioning was simulated by deliberately torquing the cannula from normal resting position (with respect to the long axis of the borescope), and holding it in position with a ring stand. Once set for the first cannula design, the positioning of the ring stand remained unchanged throughout the rest of the experiment in an attempt to simulate similar malpositioning between cannulae.

In the hypovolemic simulation, the pressure of the left atrium (LAP, also interchangeably referred to as preload) was initially set to 20mmHg. The simulation was run at fixed pump speeds of 1250, 1500, and 1750 RPM. At each pump speed, the resistance generated proximal to the heart by the Hoffman clamp was increased such that the LAP would decrease by increments

of 1mmHg. At each increment the LAP, flow and time of experiment were recorded by hand. Continuous data recording was also performed by an Iotech TB-100 DAQ board (Iotech Inc., Cleveland, OH). The LAP was repeatedly decreased until nearly complete occlusion of the cannula was observed on the monitor.

For the over-pumping simulation, the resistance of the Hoffman clamp was fixed in order to control the initial LAP, and the pump speed was then increased. The simulation was run at initial LAPs of 20, 15, and 10mmHg when set at 1200RPM. The speed was then increased by increments of 100RPM. At each increment the pump speed, flow, and time of experiment were recorded by hand. Continuous data recording was also performed by the data acquisition system. The pump speed was incrementally increased until nearly complete occlusion of the cannula was observed on the monitor.

The entire experiment was run to completion twice. Each time, a different heart was used, and the order of cannula use was changed. In addition to the recording of LAP and flow, the DAQ system recorded a “Pout”. For the first study, the Pout was measured immediately distal to the cannula. For the second study, Pout was measured distal to the outflow of the pump.



Figure 29- The beveled cannula (white) and the QVC (blue)



Figure 30-- (Left) Properly positioned cannula. (Right) Intentionally malpositioned cannula.

3.3.2.3 Analysis

Both qualitative and quantitative assessment of the cannulae were made using this setup. The reproducibility of the events generated during this study was also considered following its completion.

Qualitative

Throughout the study, videographic images of the ventricular chamber were displayed in real-time. The videos of each run were recorded to a DVD for further review. From the videos, still images were captured using VLC Media software (VideoLAN) at each increment of each study. Image saturation, brightness, and contrast were altered in order to increase the differentiation between cannula and myocardium. The state of the ventricle, cannula, seed particles, and flow fields were noted. As ventricular suction and or collapse occurred, the modality of cannula occlusion was recorded.

Quantitative

Data recorded via DAQ system was extracted as a text file from LabView and post-processed in MATLAB. The mean values the digital data recorded at each increment were compared to the hand-written data to ensure accuracy of measurements. Additionally, the continuous data recorded during suction events were plotted to illustrate the characteristics of varying suction events.

Incremental LAP and flow data were placed in Microsoft Excel for analysis. Flows recorded during the hypovolemic simulation for each orientation of each cannula were plotted versus LAP. Additionally the percentage of change in flow at each increment for a particular cannula was calculated using the following equation:

$$1) \%Change = \frac{Q_{mal} - Q_{proper}}{Q_{proper}} * 100\%$$

Where Q_{proper} is the flow recorded at a specific increment of LAP when a cannula is oriented properly, and Q_{mal} is the flow recorded for the same cannula, at the same increment of LAP, but in the sub optimal orientation. The Percentage change was then plotted versus the LAP.

Incremental data recorded during the over-pumping simulation was plotted with respect to pump speed. For this scenario, the percentage change in maximal flow, irrespective of pump speed, was calculated using the following equation:

$$2) \%Change = \frac{Q_{\max mal} - Q_{\max proper}}{Q_{\max proper}} * 100\%$$

Where $Q_{\max proper}$ is the maximal flow attained using a particular cannula in nominal orientation, and $Q_{\max mal}$ is the maximal flow using the same cannula, but oriented suboptimally.

3.3.3 Results

Qualitative

The borescope was able to provide images of the cannulae, myocardium and flow fields in both nominal and malpositioned orientations. Images acquired from the isolated heart setup elucidated the various types of suction events that occurred throughout the duration of the study.

Amberlite particles were clearly visible when passing through the LV chamber. Moving particles appear in the field of view as white streaks in the pictures shown in this section. In areas of low flow, the amberlite particles appear as bright dots instead of streaks, and would often accumulate in those areas. Flow fields generated by the QVC did not produce areas of stagnation. Individual particles were occasionally seen depositing themselves in crevices of trabeculae or at the very edge of the flare, but would not reside for long periods of time. This was true for both nominal and malpositioning. For the Beveled cannula, particle movement was only constant directly in the path of flow path between the mitral annuls and cannula orifice. For both malpositioned and nominal states particles were clearly accumulating at the apex near the wound site. Also, when malpositioned, the beveled cannula would catch particles where the tip of the inlet met the contralateral wall. Figure 31 provides an example of accumulation that was observed at the beveled tip.

In addition to flow fields, the three major modes of ventricular suction were generated (see Figure 32). The first mode is a concentric collapse. This method of collapse occurred when the walls of the ventricle were drawn radially inward in a nearly symmetric fashion around the center of the cannula orifice. Often, at the center of the concentric collapse an opening remained allowing some flow.

The second method of suction occurred when only the contralateral wall of the ventricular chamber was entrained by the cannula orifice. This entrainment occurred in two

ways: instantaneously, in a sudden and nearly total occlusion of the cannula; and gradually, where the myocardium would slowly be drawn to the cannula throughout the test and would increasingly obstruct flow.

The type of suction was dependent upon the cannula design and positioning. Resulting suction modes for each test are listed in

Table 1. Some of the results in the table are unavailable from the first study because the DVD recorder was inadvertently stopped during that portion. During several of the suction events generated by the QVC in the first attempt, and during nearly all suction events generated by QVC in second attempt, repeated occlusion followed by re-opening of the cannula inlet would occur. These oscillations would continue until one of the following happened:

1. Pump speed was reduced
2. The ventricle became continuously collapsed, or
3. LAP was increased

Figure 33 contains images of the cannulae at times of patency and at times of occlusion for all variations tested during the hypovolemia simulation of the second attempt. Figure 34 contains the corresponding images for the over-pumping simulation of the second attempt.

Quantitative

Differences in flow caused by variations in position were apparent when the incrementally recorded flows were plotted versus preload for the hypovolemia simulation. This trend was observed when flow was plotted versus speed for the over-pumping simulation as well.

For the majority of the studies, a nominally placed beveled cannula achieved higher flows than did the nominally placed QVC. The highest flows achieved for this study were 7.12 L/min and 6.6 L/min for the beveled and QVC, respectively in study #1. The highest flows achieved for this study were 6.7 L/min and 6.55 L/min for the beveled and QVC, respectively in study #2. Alteration of position had only a minor affect on flow at higher preloads. This was not so at lower preloads for the beveled design. As preload decreased, the difference in flows between improper and proper cannulation became much larger for the beveled cannula. So much so that it would drop well below the resulting flow of a malpositioned cannula. Figure 35 illustrates the

differences in flow observed between the two cannulae and their respective positioning during the second study attempt.

The Reynolds numbers calculated for the maximum flows reached for the beveled cannula and QVC cannula were 11,623, and 10,004 respectively (assuming steady, fully developed, Newtonian flow through a straight cylindrical tube). This indicates that inertial forces far exceeded viscous forces, and that flows were fully turbulent at maximal flow. Table 2 shows the resulting Reynolds numbers, and critical flows calculated for water and blood, which indicate the maximum values at which fully laminar flow will still be observed.

The same trend was observed during the over-pumping simulation. The beveled cannula could reach slightly higher flows before experiencing a suction event than could the QVC when both were in nominal states. However, once again the resulting flows generated by the misaligned beveled cannula dropped well below the resulting flows of the misaligned flared design. Figure 36 illustrates the decline in attainable flows from the second test run as pump speed is increased with a malpositioned pump.

Calculation of the relative changes (percentage change in flow) caused by changing orientation could only be performed at increments where both Q_{proper} and Q_{mal} could be measured. This narrowed the range of settings that could be compared between cannula designs. Even so, enough measurements could be taken to adequately illustrate the relative changes in flow for each simulation and the effect that design had on positional sensitivity. Figure 37 shows that in the 2nd attempt of the hypovolemic simulation the beveled cannula experienced a drop in flow of nearly 48% at a LAP of 5mmHg due to malposition. At that same condition, using the QVC, a drop of less than 5% occurred. The relative changes in maximal flows attained during the over-pumping simulations showed that there was as much as a 29.5% decrease in Q_{max} in study #2 and 34.2% for study #1 for the beveled cannula due to poor positioning, while there was at most an 8.2% decrease when the QVC was malpositioned for study #2 and at most a 7.3% decrease in study #1. Figure 37 and Figure 38 illustrate the relative changes in flow of both experiments.

Digitally acquired data, as shown in Figure 39, could be used to identify when suction occurred, even when a written value could not be accurately determined, or in the case that the images had not been recorded. The data could identify whether or not the occlusion was complete and whether or not there were oscillations. Figure 40 shows that at least two variations

in oscillation occurred. The first is identifiable because its minimal flow is still above zero. The second intermittently ceases flow, and can even generate negative flows through the pump.

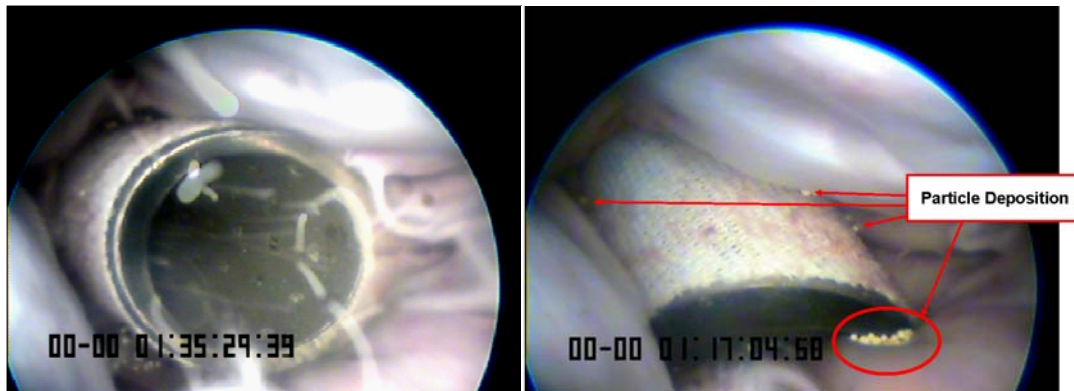


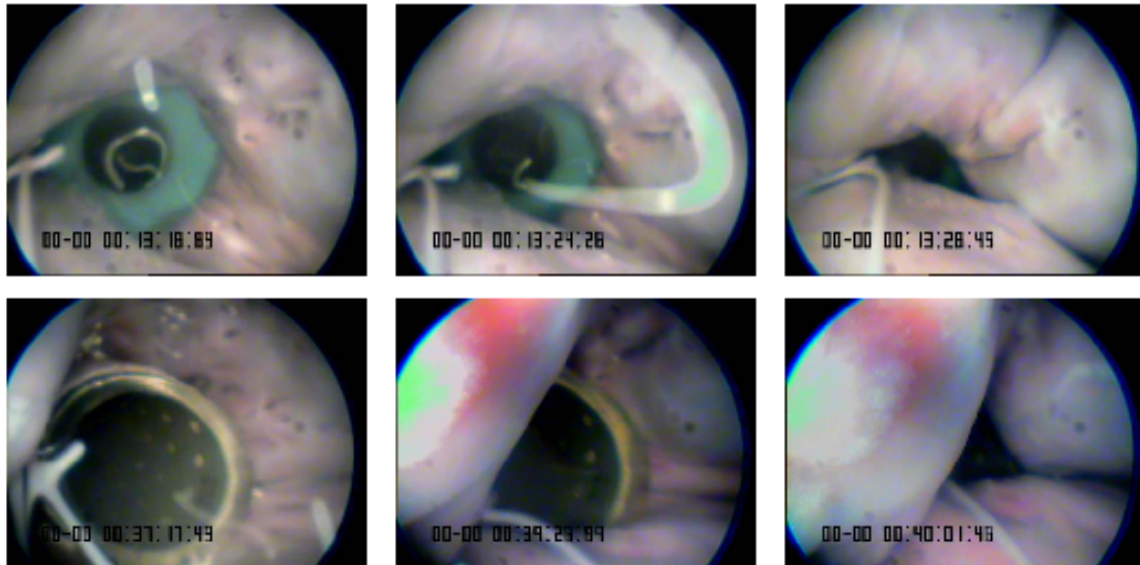
Figure 31-Particle flow fields generated at a patent beveled cannula inlet (left) and deposition surrounding a malpositioned beveled cannula (right).

Table 1-Modes of collapse which occurred for each setting

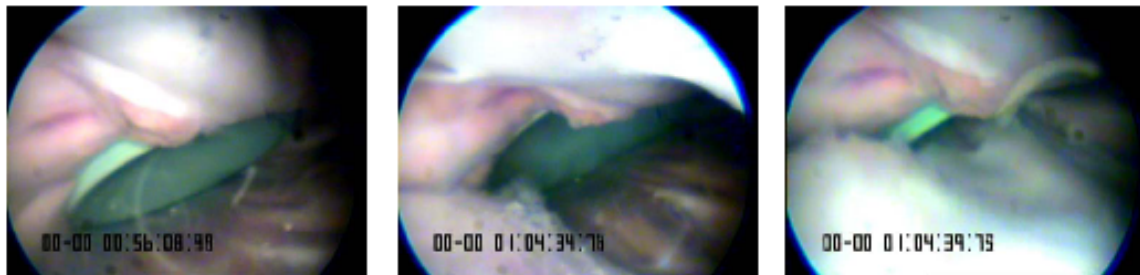
Position	Fixed Parameter	Parameter value	BEV		QVC	
			Attempt #1	Attempt #2	Attempt #1	Attempt #2
Proper	Speed	1250 RPM	NA	Concentric	<u>Concentric</u>	<u>Concentric</u>
Mal	Speed	1250 RPM	Concentric	Gradual Entrainment	Concentric	Instantaneous Entrainment_*
Proper	Speed	1500 RPM	Concentric	Concentric	<u>Concentric</u>	<u>Concentric</u>
Mal	Speed	1500 RPM	Gradual Entrainment	Gradual Entrainment	Concentric	<u>Instantaneous Entrainment</u>
Proper	Speed	1750 RPM	Concentric	Concentric	<u>Concentric</u>	<u>Concentric</u>
Mal	Speed	1750 RPM	Gradual Entrainment	Gradual Entrainment	NA	<u>Instantaneous Entrainment</u>
Proper	Initial preload	20 mmHg	Concentric	Concentric	<u>Concentric</u>	Concentric
Mal	Initial preload	20 mmHg	Gradual Entrainment	Gradual Entrainment	NA	<u>Instantaneous Entrainment</u>
Proper	Initial preload	15 mmHg	Concentric	Concentric	Concentric	<u>Concentric</u>
Mal	Initial preload	15 mmHg	Gradual Entrainment	Gradual Entrainment	NA	<u>Instantaneous Entrainment</u>
Proper	Initial preload	10 mmHg	Concentric	Concentric	Concentric	<u>Concentric</u>
Mal	Initial preload	10 mmHg	Gradual Entrainment	Gradual Entrainment	NA	<u>Instantaneous Entrainment</u>
NA=Image Not Available			Mal= malpositioned			
			<i>Oscillation occurred if italicized and underlined</i>			

* Run was ceased prior to oscillation; though observation of ventricle state indicates that a repeated collapse may have occurred if run had been allowed to continue beyond first event.

Concentric Collapse



Instantaneous Entrainment



Gradual Entrainment

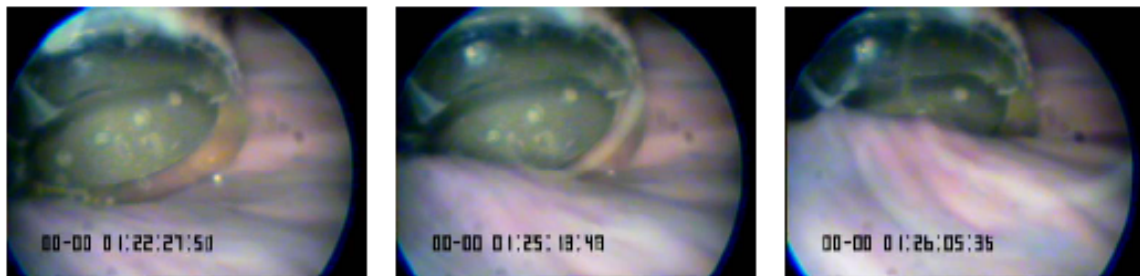


Figure 32-Still images captured from borescopic video which illustrate the progression of the various modes of suction that occurred during the study.

Hypovolemic Simulation

(Fixed speed, decreasing LAP)

Nominal

Suboptimal



Figure 33- Still images acquired from the simulation of hypovolemia

Over-pumping Simulation

(Fixed Initial Preload , Increasing pump Speed)

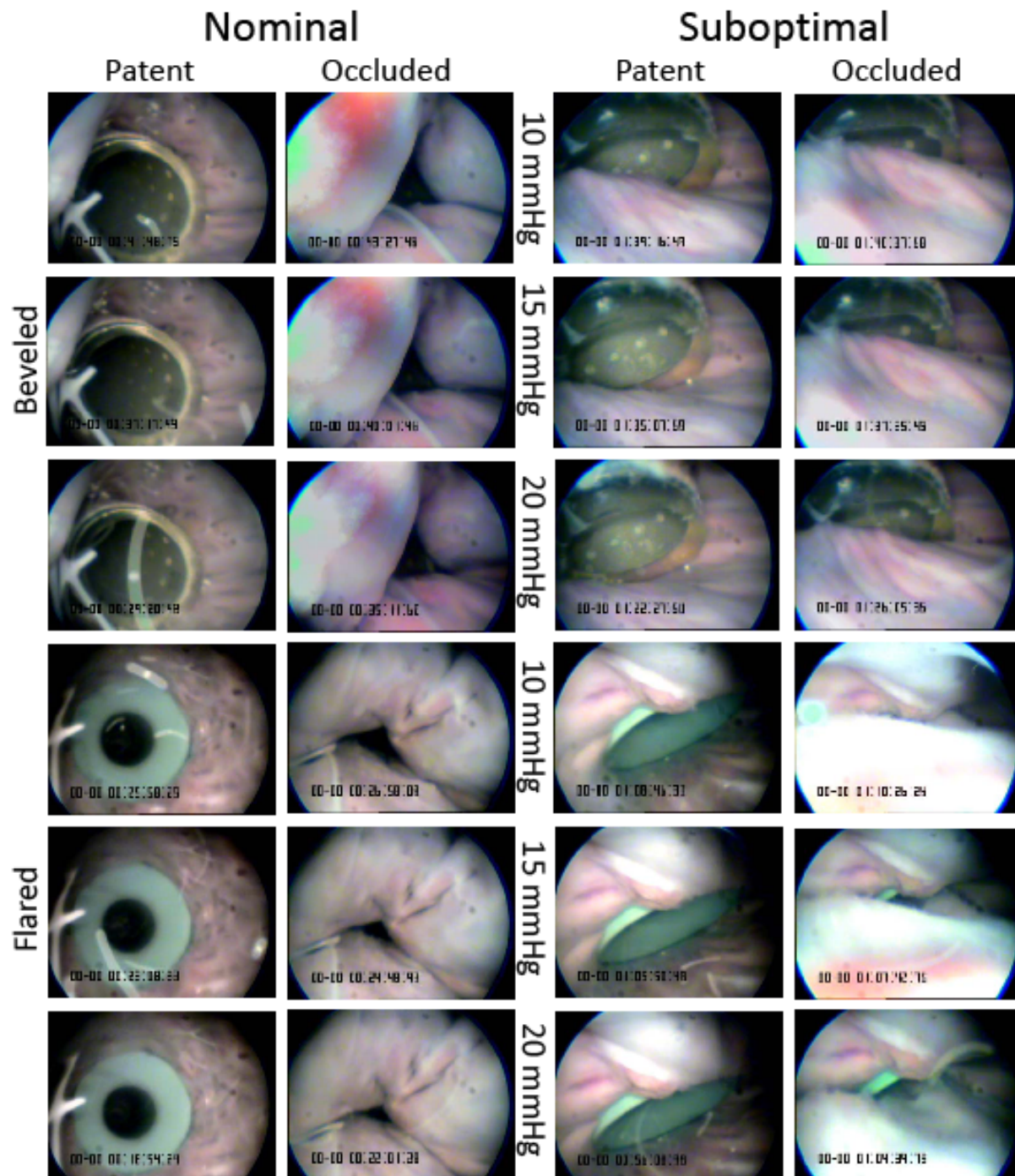


Figure 34-Still images of the over-pumping simulation

Comparison of Cannulae in Proper and Malpositioned States Fixed Speed of 1250 RPM

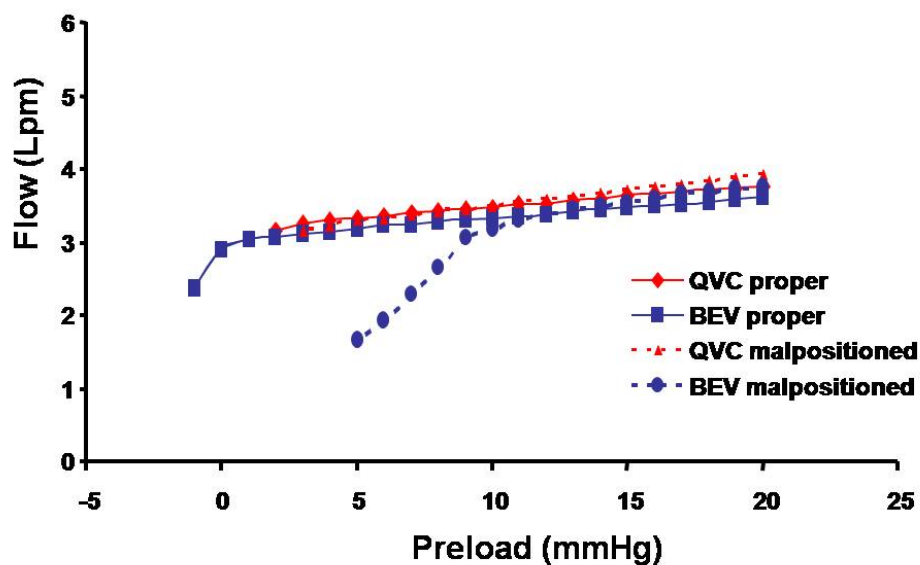


Figure 35- Pressure versus flow during the hypovolemic simulation in second study with pump speed fixed to 1250 RPM.

Comparison of Cannulae in Proper and Malpositioned States Fixed initial Preload of 20 mmHg at 1200 RPM

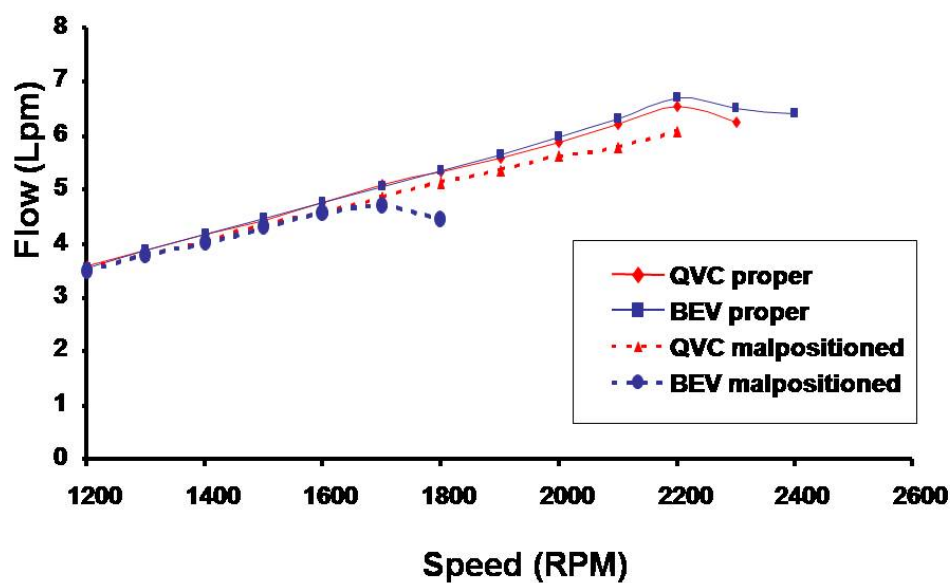


Figure 36- Flow versus speed data for properly and improperly placed cannula during the over-pumping simulation in second study at a fixed initial LAP of 20mmHg.

Table 2-Assumed values and resulting Reynolds numbers for cannulae

	Beveled Cannula	QVC
Viscosity (μ)- Water	.01 P	.01 P
Viscosity (μ)- Blood	.03 P	.03 P
Density (ρ)-Water	1.00 g/cm ³	1.00 g/cm ³
Density (ρ)- Blood	1.05 g/cm ³	1.05 g/cm ³
Cannula Internal Diameter	13 mm	14 mm
Reynolds Number (max flow)	11623	10004
Q(laminar*)-Water	1.22 L/min	1.32 L/min
Q(laminar*)- Blood	3.5 L/min	3.77 L/min

*Assumed Reynolds number of 2000 to determine critical value at fully laminar flow

Comparison of Cannulae in Proper and Malpositioned States

%Change in flow due to malposition at 1250 rpm

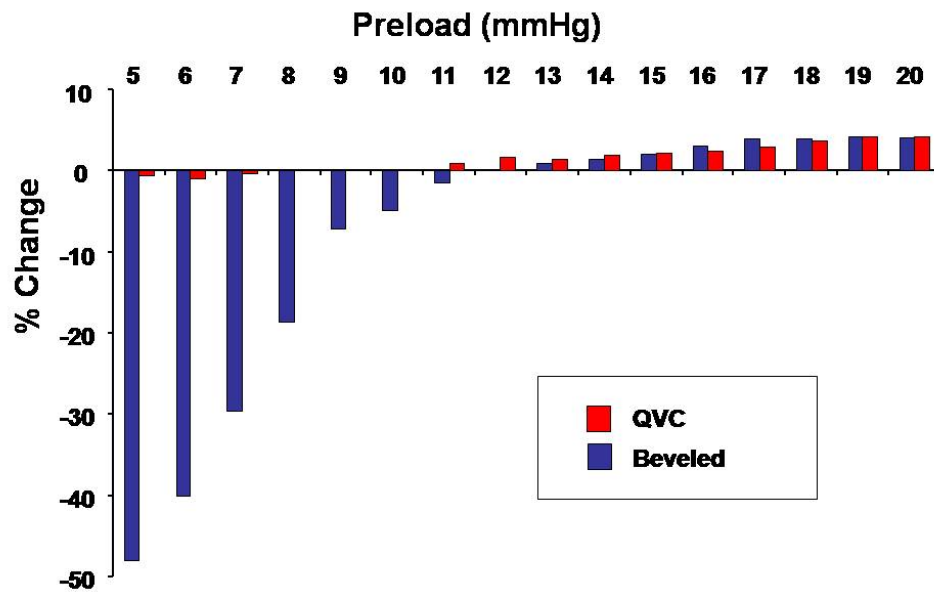


Figure 37-Percentage change in flow for the hypovolemic simulation in second study at a fixed speed of 1250 RPM.

Comparison of Cannulae in Proper and Malpositioned States **%Change in flow due to malposition**

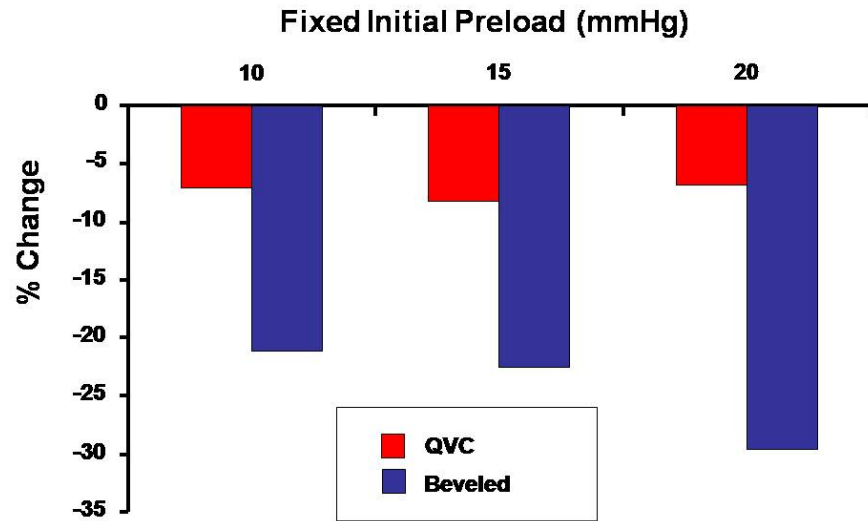


Figure 38- Percent change in maximal attainable flow (regardless of speed) measured during the over-pumping simulation of the second study.

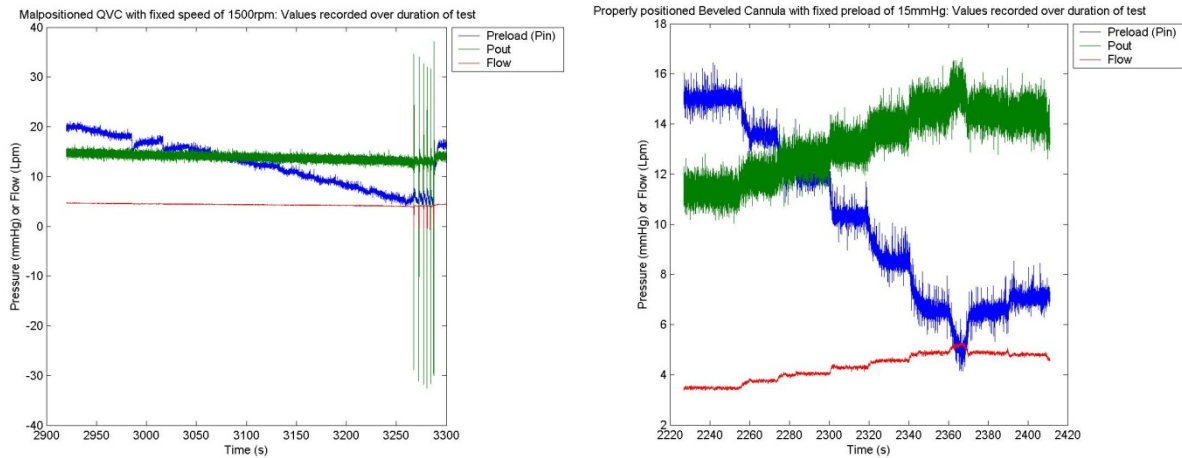


Figure 39- Examples of the progression of the data acquired during a test run (study attempt #2). (Left) Progression of a hypovolemic study, concluding with an oscillation. (Right) Progression of an over-pumping study.

Suction Event Data

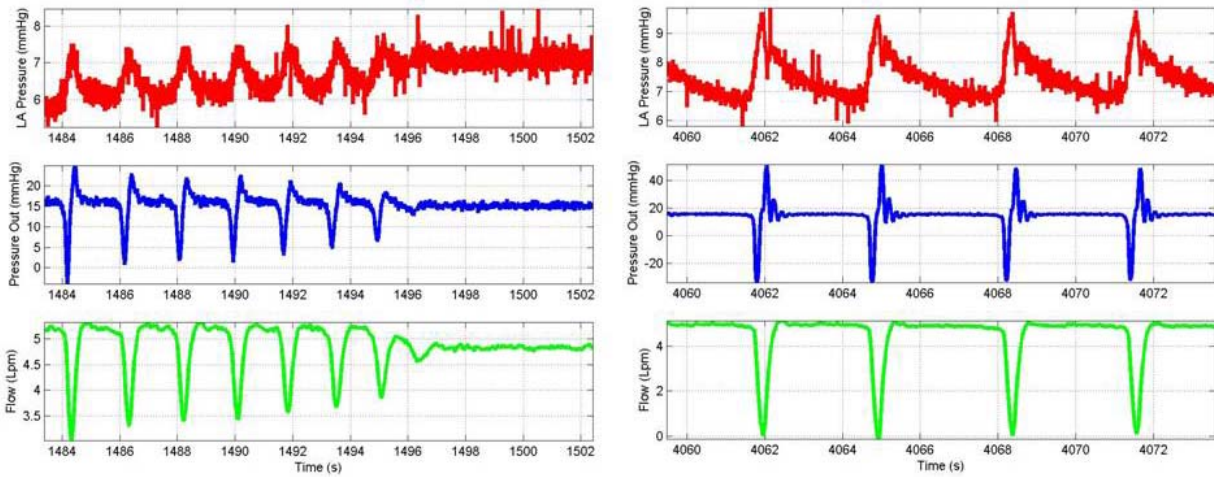


Figure 40-Examples of variations of Oscillation. (Left) incomplete occlusion with dampening. (Right) Total occlusion.

3.3.4 Discussion

This study was able to visualize various forms of VAD-induced left ventricular suction in-situ, and was able to evaluate the performance of differing cannula designs in favorable and unfavorable conditions. The study demonstrated that positioning of the cannula can influence the resulting flows generated by a continuous flow LVAD. It also demonstrated that design of the cannula can decrease its sensitivity to malposition. In the case of this study, the flared, form-fitting cannula design was less sensitive to malposition than a beveled cannula.

The results that were obtained also raised more questions that could be further explored. For instance, one could ask if certain suction events limited to specific cannula designs or orientations. If it does then those traits could be included in future VAD control algorithms to not only detect suction, but to detect what kind of suction may be occurring. Another phenomenon that was noticed was that at least initially, a malpositioned cannula provided higher flows than did the “nominally” placed cannula. One could explore what a truly “nominal cannula position is. This would require a larger number of experiments to be conducted so that statistical analysis could be performed.

However, before more experiments are undertaken some limitations to this setup and data must be addressed. First and foremost, the heart is not beating. By the time the ovine heart has arrived at the testing facility, the window of time during which the heart can be re-animated has passed. Although some patients are a-systolic, most patients who have a continuous flow LVAD do retain some pulsatility due to native myocardial function. The interactions between the cannula and the endocardium may differ depending on the state of the ventricle. This leads to the next limitation- the state of the ventricle. The heart, which is now composed of dead tissue, is constantly dilating due to the preload generated by the elevated reservoir. As time elapsed through both study attempts, the LV became more dilated. While this may seem appealing, because LVADs are implanted in patients with failing, dilated LVs, it makes comparisons between two different cannula types difficult. One must be careful when comparing absolute flows obtained by the different cannulae. This is because as the heart dilates, it creates a larger volume for the LVAD to unload. This study attempted to address this limitation in two ways: the first method was by alternating which cannula was studied first. In study number 1 the QVC was inserted first, and encountered a smaller LV volume. The beveled cannula was inserted first for the second study attempt. The other method was to use relative change as a means of comparison. This method normalized the flow that resulted from malpositioning against the initial flow that was obtained. If future test runs were to take place, pre-conditioning of the heart should be considered.

Ultimately, in order to make this study more accurate and versatile, a heart would need to still be beating, and the setup should preserve the integrity of the myocardial tissue. In 2007 van Tuijl et al presented an abstract at the American Society of Artificial Internal Organs conference where a porcine heart was harvested at a slaughterhouse, the LV was cannulated, the heart was then re-animated and the hemodynamic characteristics studied.[21] Taking this idea even further, one could attempt to perform the study in-vivo, using a system like that of Mihaljevic et al. who maintained systemic organs of a porcine model using cardiopulmonary bypass, and connected the heart to a separate circuit that replaced blood with a transparent crystalloid solution so that cardioscopes could be employed to evaluate cardiac anatomy.[22] This would produce a preserved, beating heart that would be ideal for further cannulation studies.

4.0 CONCLUSIONS

The novel QVC was developed to be positionally insensitive, to conform to the geometry of the LV, to facilitate greater ease of proper and reproducible insertion, to generate hemodynamically favorable flow, and to be less susceptible to collapse under mild suction conditions.

In-silico and ex-vivo anatomic fit studies proved that the cannula will not interfere with essential ventricular features such as primary chordae or the papillary muscles. The CT reconstructions proved to be a valuable means of assessing the proposed cannula designs before actually fabricating the final version. The ex-vivo fit study confirmed that the flare would fit flush against the endocardial surface, even when torqued at extreme angles.

Ease of proper insertion was apparent during the anatomic fit study, the pullout study, and the suction study. The internal flare was flexible enough that its diameter could be reduced to that of the rest of the shaft with a pair of clamps, while at the same time requiring a significant amount of force to be removed following deployment.

Finally, the suction study proved to be a successful system for determining how various cannula designs would interact with an LV chamber when oriented in optimal and suboptimal conformations in both ideal and adverse conditions. The system proved beyond a reasonable doubt that the cannula was far less positionally sensitive than the beveled cannula design, and that it also produced hemodynamically favorable flows with fewer areas of stagnation that could potentially promote thrombus formation.

4.1 PROPOSED MODIFICATIONS OF CANNULA

While the findings from the evaluation of this novel cannula design were promising and indicative of a conformal cannula design's superiority over conventional rigid-tube cannulae, there were flaws in the design that should be addressed in the next generation of cannula.

4.1.1 Facilitation of Hemostasis

In its current form, the external clasp, internal flare design does not facilitate suturing to the myocardium. The intension of this design was to remove the need for suturing altogether; however, as observed during experiments, the myocardium may stretch with repeated insertions, increasing the diameter of the core at the apex and preventing hemostasis at the wound site. In the operating room, repeated insertions may not occur as often as in the lab setting; however, if a cannula size was not accurate and a replacement was needed, or if the diameter of the incision made by the surgeon was too great, the need to anchoring may be required.

Another addition that should be made to the cannula is the incorporation of textured material, such as velour, to the area of the shaft between the external clasp and internal flare. Adding this to the design will promote tissue ingrowth at the wound site.

4.1.2 Sizing

Patients come in all shapes and sizes. The QVC cannot be one-size-fits-all. There should be several variations built that provide adequate selections for the surgeon who is performing the implant. The surgeon should be able to make his or her decision based on desired flows, as well as measurements taken by non-invasive means such as transthoracic, echocardiography.

4.2 CONTRAINDICATIONS FOR USE

As with many medical devices, there are contraindications for use of this cannula design. As was noted during ex-vivo anatomic fit studies, certain animal models were ruled out for use because of the inability of the QVC to completely deploy in the presence of hypertrophied myocardium. Therefore this cannula design is not suited for patients with hypertrophic cardiomyopathy.

4.3 FUTURE STUDIES

Before one can truly label the QVC as “quintessential” there are several studies that must be performed. Particularly, chronic in-vivo studies must show that the QVC is effective at generating adequate flows over a long period of time. One concern would be obstruction of the cannula over time, due to neointimal growth, which may envelop the flare.

Another crucial study would be to determine if the force generated by the clasp concept would cause ischemia at the apex that may be harmful to the surrounding and otherwise viable myocardium.

Finally, studies of the high-memory polymer must be performed to ensure that the blood contacting surface is non-thrombogenic.

APPENDIX A

ADDITIONAL GRAPHS FROM SECOND STUDY

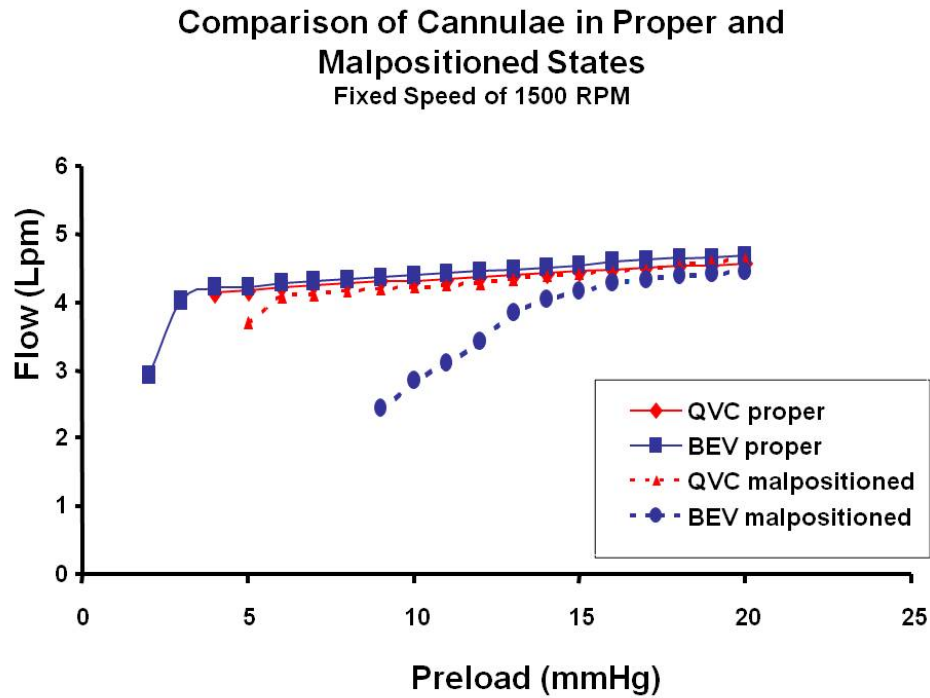


Figure 41-Pressure versus flow during the hypovolemic simulation in second study with pump speed fixed to 1500 RPM.

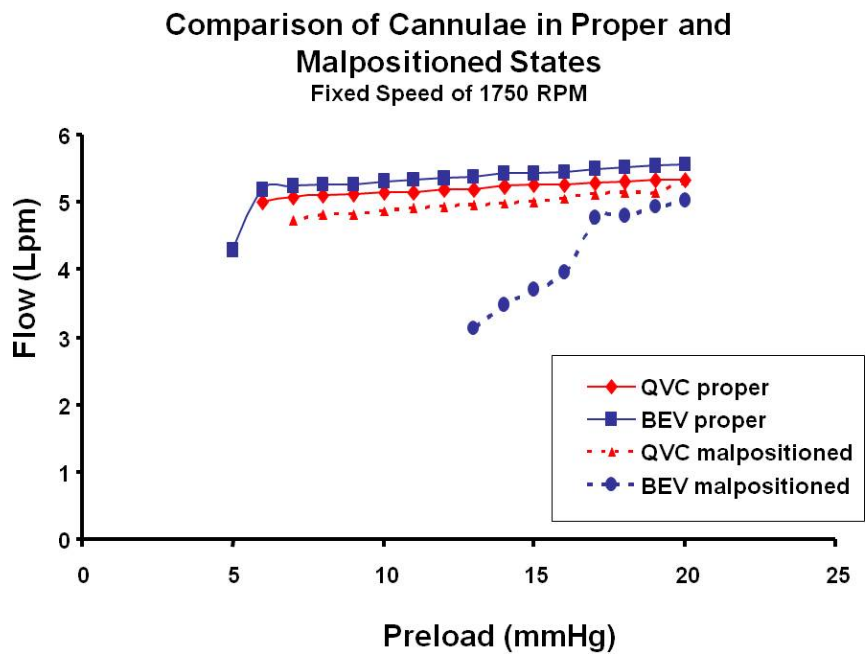


Figure 42-Pressure versus flow during the hypovolemic simulation in second study with pump speed fixed to 1750 RPM.

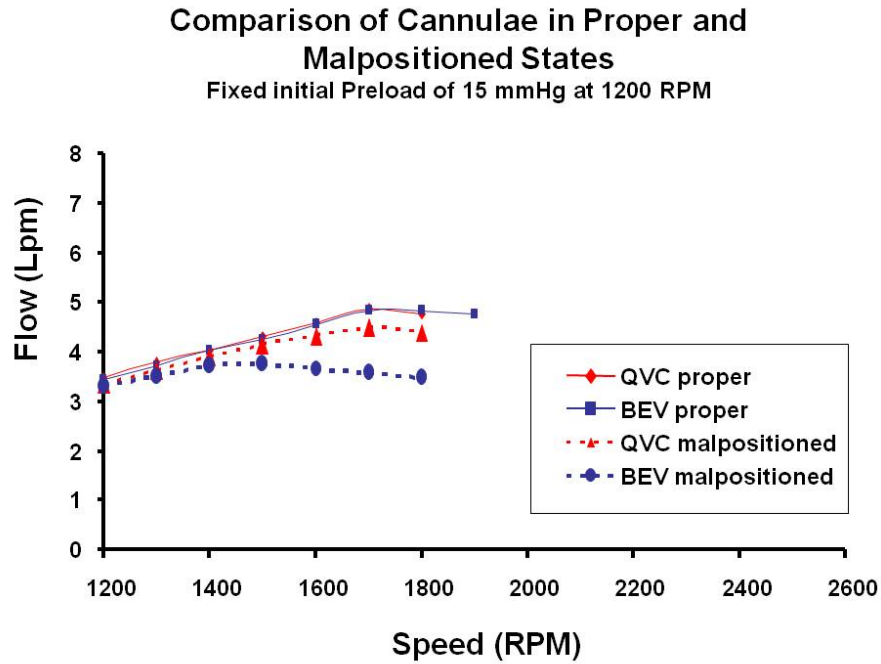


Figure 43-Flow versus speed data for properly and improperly placed cannula during the over-pumping simulation in second study at a fixed initial LAP of 15mmHg

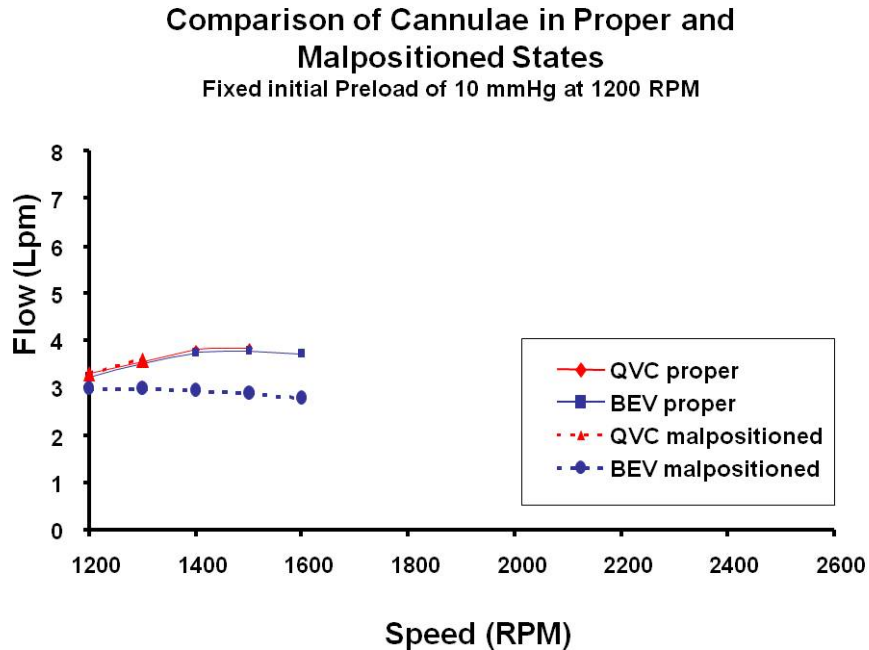


Figure 44-Flow versus speed data for properly and improperly placed cannula during the over-pumping simulation in second study at a fixed initial LAP of 10mmHg

Comparison of Cannulae in Proper and Malpositioned States

% Change in flow due to malposition at 1500 rpm

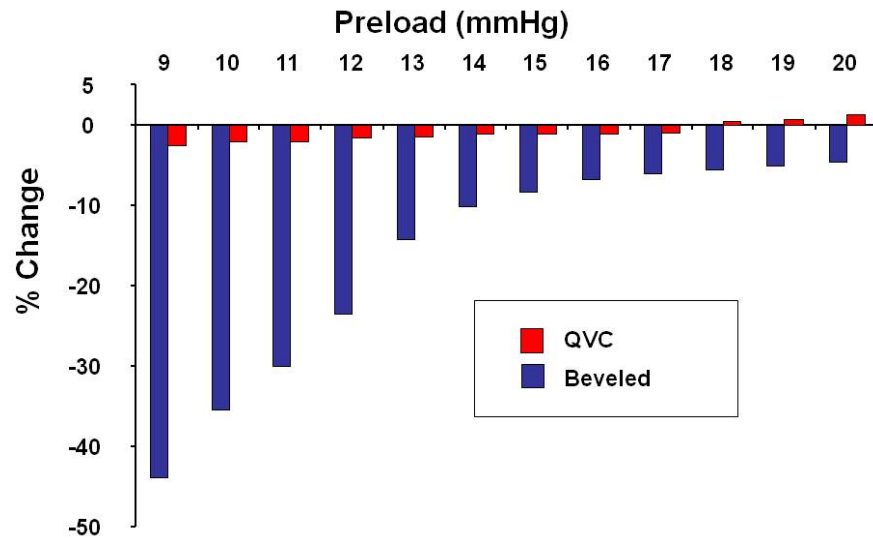


Figure 45-Percentage change in flow for the hypovolemic simulation in second study at a fixed speed of 1500 RPM.

Comparison of Cannulae in Proper and Malpositioned States

% Change in flow due to malposition at 1750 rpm

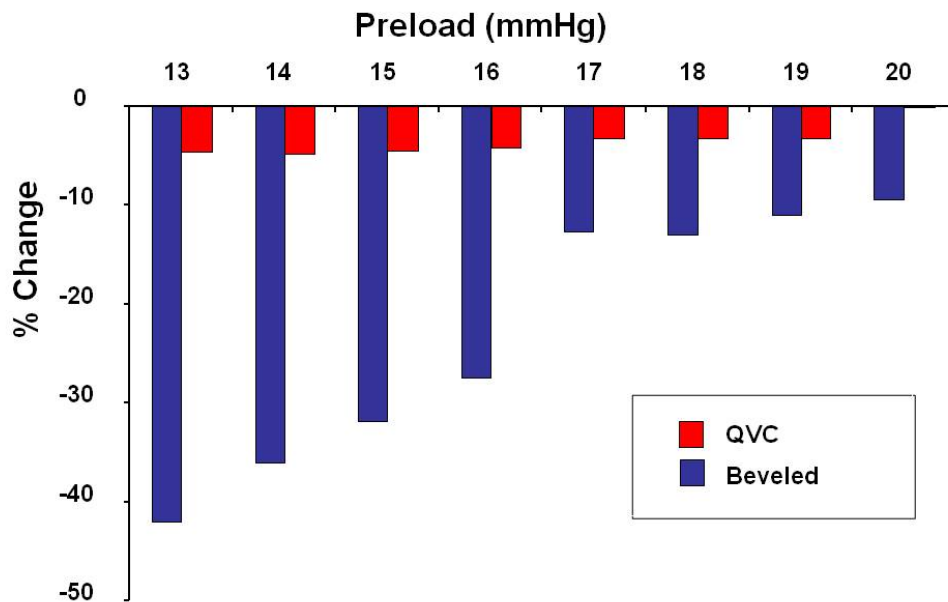


Figure 46-Percentage change in flow for the hypovolemic simulation in second study at a fixed speed of 1750 RPM.

BIBLIOGRAPHY

1. Rosamond, W., et al., *Heart disease and stroke statistics--2008 update: a report from the American Heart Association Statistics Committee and Stroke Statistics Subcommittee*. Circulation, 2008. **117**(4): p. e25-146.
2. Hetzer, R., et al., *Bridging-to-recovery*. Ann Thorac Surg, 2001. **71**(3 Suppl): p. S109-13; discussion S114-5.
3. Simon, M.A., et al., *Myocardial recovery using ventricular assist devices: prevalence, clinical characteristics, and outcomes*. Circulation, 2005. **112**(9 Suppl): p. I32-6.
4. Holman, W.L., et al., *Left atrial or ventricular cannulation beyond 30 days for a Thoratec ventricular assist device*. ASAIO J, 1995. **41**(3): p. M517-22.
5. Lohmann, D.P., et al., *Left ventricular versus left atrial cannulation for the Thoratec ventricular assist device*. ASAIO Trans, 1990. **36**(3): p. M545-8.
6. Badiwala, M.V., H.J. Ross, and V. Rao, *An unusual complication of support with a continuous-flow cardiac assist device*. N Engl J Med, 2007. **357**(9): p. 936-7.
7. Amin, D.V., et al., *Induction of ventricular collapse by an axial flow blood pump*. ASAIO J, 1998. **44**(5): p. M685-90.
8. Reesink, K., et al., *Suction due to left ventricular assist: implications for device control and management*. Artif Organs, 2007. **31**(7): p. 542-9.
9. Watanabe, K., et al., *Development of a flexible inflow cannula with titanium inflow tip for the NEDO biventricular assist device*. ASAIO J, 2004. **50**(4): p. 381-6.
10. Hetzer, R., *Proceedings of the 4th Berlin Symposium on Mechanical Circulatory Support*. J Card Surg, 2006. **21**: p. 512-520.
11. Snyder, *Preclinical Biocompatibility Assessment of Cardiovascular Devices in Bioengineering*. 2006, University of Pittsburgh.
12. Miyake, Y., et al., *Left ventricular mobile thrombus associated with ventricular assist device: diagnosis by transesophageal echocardiography*. Circ J, 2004. **68**(4): p. 383-4.

13. Votapka, T.V., et al., *Left ventricular cannula obstruction in a patient with previous ventricular aneurysmectomy*. Ann Thorac Surg, 1994. **58**(4): p. 1182-4.
14. Griffith, B.P., et al., *HeartMate II left ventricular assist system: from concept to first clinical use*. Ann Thorac Surg, 2001. **71**(3 Suppl): p. S116-20; discussion S114-6.
15. Vollkron, M., et al., *Suction events during left ventricular support and ventricular arrhythmias*. J Heart Lung Transplant, 2007. **26**(8): p. 819-25.
16. Ferreira, A., et al., *A discriminant-analysis-based suction detection system for rotary blood pumps*. Conf Proc IEEE Eng Med Biol Soc, 2006. **1**: p. 5382-5.
17. Choi, S., J.R. Boston, and J.F. Antaki, *Hemodynamic controller for left ventricular assist device based on pulsatility ratio*. Artif Organs, 2007. **31**(2): p. 114-25.
18. Vollkron, M., et al., *Development of a suction detection system for axial blood pumps*. Artif Organs, 2004. **28**(8): p. 709-16.
19. Antaki, J.F., et al., *An improved left ventricular cannula for chronic dynamic blood pump support*. Artif Organs, 1995. **19**(7): p. 671-5.
20. Curtis, A.S., et al., *Novel ventricular apical cannula: in vitro evaluation using transparent, compliant ventricular casts*. ASAIO J, 1998. **44**(5): p. M691-5.
21. *ASAIO Bioengineering/Tissue Engineering Abstracts*. ASAIO Journal, 2007. **53**(2): p. A1-69.
22. Mihaljevic, T., et al., *Beating heart cardioscopy: a platform for real-time, intracardiac imaging*. Ann Thorac Surg, 2008. **85**(3): p. 1061-5.